

Message-Passing Receiver for Joint Channel Estimation and Decoding in 3D Massive MIMO-OFDM Systems

Sheng Wu, *Member, IEEE*, Linling Kuang, *Member, IEEE*,

Zuyao Ni, Defeng (David) Huang, *Senior Member, IEEE*,

Qinghua Guo, *Member, IEEE*, and Jianhua Lu, *Fellow, IEEE*

Abstract

In this paper, we address the message-passing receiver design for the 3D massive MIMO-OFDM systems. With the aid of the central limit argument and Taylor-series approximation, a computationally efficient receiver that performs joint channel estimation and decoding is devised by the framework of expectation propagation. Specially, the local belief defined at the channel transition function is expanded up to the second order with Wirtinger calculus, to transform the messages sent by the channel transition function to a tractable form. As a result, the channel impulse response (CIR) between each pair of antennas is estimated by Gaussian message passing. In addition, a variational expectation-maximization (EM)-based method is derived to learn the channel power-delay-profile (PDP). The proposed joint

This work was partially supported by the National Nature Science Foundation of China (Grant Nos. 91338101, 61231011, and 91438206), the National Basic Research Program of China (Grant No. 2013CB329001), and Tsinghua University Initiative Scientific Research Program (Grant No. 20131089219).

Sheng Wu, Linling Kuang and Zuyao Ni are with the Tsinghua Space Center, Tsinghua University, China (e-mail: {thuraya, kll, nzy}@tsinghua.edu.cn).

Defeng (David) Huang is with the School of Electrical, Electronic and Computer Engineering, The University of Western Australia, Australia (e-mail: david.huang@ee.uwa.edu.au).

Q. Guo is with the School of Electrical, Computer and Telecommunications Engineering, University of Wollongong, Australia, and is also with the School of Electrical, Electronic and Computer Engineering, The University of Western Australia, Australia (e-mail: qinghua.guo@uow.edu.au).

Jianhua Lu is with the Department of Electronic Engineering, Tsinghua University, China (e-mail: lhh-dee@mail.tsinghua.edu.cn).

algorithm is assessed in 3D massive MIMO systems with spatially correlated channels, and the empirical results corroborate its superiority in terms of performance and complexity.

Index Terms

Expectation Propagation, Joint Channel Estimation and Decoding, 3D Massive MIMO, Message Passing, OFDM.

I. INTRODUCTION

Recently, massive multiple-input multiple-output (MIMO) systems with tens to hundreds of antennas at the base-station (BS) have gained significant attention [1]–[4]. It has been proved that massive MIMO systems can scale down transmit power as well as increase spectrum efficiency by orders of magnitude [2]. One of the tasks in massive MIMO systems is estimating the channel impulse response (CIR) for each transmit-receive link, since high data rates and energy efficiency can only be achieved when CIR is known [5]. In contrast to the conventional MIMO systems employing a small number of antennas, there are a large number of channels need to be estimated. The pilot overhead required for channel estimation is proportional to the number of transmit antennas, which can be excessive in massive MIMO systems [6]. In the meantime, the available resources for training are restricted by the channel coherence time. On the other hand, the energy consumption by baseband processing grows with the number of antennas, which may obliterate the advantage of massive MIMO systems in energy efficiency. Thus, low-complexity channel estimation with high accuracy and reduced overhead is critical to massive MIMO systems.

Iterative receivers that jointly estimate the channel coefficients and detect the data symbols are able to provide more accurate channel estimation with less training overhead [7]–[12]. Factor graph and sum-product algorithm (SPA) [13] have been used as a unified framework for iterative joint data detection, channel estimation, interference cancellation, and decoding [14], [15]. However, exact SPA for joint channel estimation and decoding is computationally infeasible. To overcome this problem, various message-passing algorithms based on approximate inference have been proposed [8], [16]–[23]. In existing approaches, the message passing strategies include loopy belief propagation (LBP) [8], [16], [19]–[21], variational methods [17], [23], [24], and a hybrid of both [18], [22].

LBP has a high complexity when applied to graphical models that involve both discrete and continuous random variables. This has been addressed by merging the SPA with the expectation-maximization (EM) algorithm [19] or approximating the messages of SPA with Gaussian messages [8], [19], [20], [25]. Variational inference methods have been applied to MIMO receivers for joint detection, channel estimation, and decoding [17]. In [18], Riegler *et al.* derived a generic message-passing algorithm that merges belief propagation (BP) with the mean-field (MF) approximation (BP-MF), and applied it to joint channel estimation and decoding in single-input single-output orthogonal frequency division multiplex (OFDM) systems and MIMO-OFDM systems [18], [22], [26]. The BP-MF has to learn the noise precision to take into account the residual interference from other users even when the noise power is known [27], [28], as the channel transition functions are incorporated into the MF part [18], [22], [26]. Otherwise, the uncertainty of residual interference is completely ignored, and the likelihood function associated with the messages extracted from observations tends to overwhelm the *a priori* probability. Besides, the BP-MF requires high computational complexity as large matrices need to be inverted to estimate channel frequency response (CFR) [18], and thereby it is only feasible in the case of a few antennas and subcarriers. We note that there is a low-complexity version of the BP-MF algorithm proposed in [29], but its performance is inferior. The degraded performance may be due to the unrealistic assumption that groups of contiguous channel weights in frequency-domain obey a Markov model.

To achieve joint channel estimation and decoding for massive MIMO systems using OFDM modulation in frequency-selective channels, the receiver needs to complete three tasks: decoupling frequency-domain channel coefficients and data symbols from noisy observations, decoding, and channel estimation. Via central-limit theorem and moment matching, an approximate BP has been derived in [8], [16] and [21]. Despite its superior performance, the approximate BP bears a heavy computation burden: it needs to take a large number of moment-matching operations, each being highly complicated. In this paper, we use the framework of expectation propagation (EP) [30] to derive an efficient message-passing algorithm. Specifically, at the channel transition functions, we use the central-limit theorem to efficiently obtain the beliefs of frequency-domain channel coefficients and the beliefs of data symbols, and then employ a quadratic approximation to project them into the Gaussian family. In the meantime, the expectation propagation principle is applied to the symbol-variable nodes. As the beliefs of frequency-domain channel coefficients

are now in the form of Gaussian family, a Gaussian message passing based estimator [31] can be employed, which exploits the fact that the CFR is the Fourier transformation of the CIR. Furthermore, using the beliefs of time-domain channel taps, the unknown power-delay-profile (PDP) can be learned by variational expectation maximization. We note that Parker *et al.* applied central-limit theorem and Taylor-series approximations to formulate a bilinear generalized approximate message-passing algorithm for the SPA in the high dimensional limit [32], but its scope is different from that of this work.

The proposed scheme of joint channel estimation and decoding is assessed in 3D massive MIMO systems with spatially correlated channels. Experiments show that its performance is within 1 dB of the known-channel bound in both a 64×8 MIMO system and a 16×8 MIMO system, and outperforms the performance of BP-MF by 0.4 dB in the 16×8 MIMO system, the low-complexity version of BP-MF by 1.2 dB in the 64×8 MIMO system and 1.6 dB in the 16×8 MIMO system. On the other hand, the complexity of the proposed algorithm is a small percentage of that of BP-MF and $\frac{1}{3}$ of that of the low-complexity version of BP-MF.

The remainder of this paper is organized as follows. The system model is described in Section II. In Section III the message passing for joint detection and decoding is detailed. Complexity comparisons are shown in Section IV, and numerical results are provided in Section V, followed by conclusions in Section VI.

Notation: Lowercase letters (e.g., x) denote scalars, bold lowercase letters (e.g., \mathbf{x}) denote column vectors, and bold uppercase letters (e.g., \mathbf{X}) denote matrices. The superscripts $(\cdot)^\top$, $(\cdot)^\mathsf{H}$ and $(\cdot)^*$ denote the transpose operation, Hermitian transpose operation, and complex conjugate operation, respectively. Also, $\text{diag}\{\mathbf{x}\}$ denotes a square diagonal matrix with the elements of vector \mathbf{x} on the main diagonal; $\mathbf{X} \otimes \mathbf{Y}$ denotes Kronecker product of \mathbf{X} and \mathbf{Y} ; \mathbf{I} denotes an identity matrix; and $\ln(\cdot)$ denotes the natural logarithm. Furthermore, $\mathcal{N}_{\mathbb{C}}(x; \hat{x}, \nu_x) = (\pi \nu_x)^{-1} \exp(-|x - \hat{x}|^2 / \nu_x)$ denotes the Gaussian probability density function (PDF) of x with mean \hat{x} and variance ν_x ; and $\text{Gam}(\gamma; \alpha, \beta) = \beta^\alpha \gamma^{\alpha-1} \exp(-\beta\gamma) / \Gamma(\alpha)$ denotes the Gamma PDF of γ with shape parameter α and rate parameter β , where $\Gamma(\cdot)$ is the gamma function. Finally, \propto denotes equality up to a constant scale factor; $\mathbf{x} \setminus x_{tnk}$ denotes all elements in \mathbf{x} but x_{tnk} ; and $\mathbb{E}_{p(x)}\{\cdot\}$ denotes expectation with respect to distribution $p(x)$.

II. SYSTEM MODEL

We consider the uplink of a massive MIMO system where N single antenna users communicate with a BS simultaneously. The BS employs a uniform planar array (UPA) consisting of $M = (D \times W) \gg N$ antennas distributed across D rows and W columns. Frequency-selective block-fading channels are assumed, and OFDM is employed to combat multipath interference.

A. Channel Model

The CIR between the n th user and the m th receive antenna is denoted by $\mathbf{h}_{mn\cdot} = [h_{mn1} \cdots h_{mnL}]^\top$, where h_{mn_l} is the l th path gain and L is the maximum channel spread. Let $\mathbf{h}_{\cdot nl} = [h_{1nl} \cdots h_{Mnl}]^\top$ denote gain vector of the l th paths between user n and all the M receive antennas at the BS. Due to close antenna spacing at the BS, we can assume that the M CIRs between the user n and all the M receive antennas at the BS follow an identical PDP $\{\mathbb{E}\{|h_{mn_l}|^2\} \triangleq \alpha_{nl}, \forall m\}$. We can also assume that the transmit antennas from different users are spatially uncorrelated. Accordingly, the Kronecker spatial fading correlation model for the gain vector $\mathbf{h}_{\cdot nl}$ is given by [33]

$$\mathbf{h}_{\cdot nl} = \mathbf{R}_{nl}^{\frac{1}{2}} \mathbf{h}_{nl}^{\text{iid}}, \quad (1)$$

where $\mathbf{R}_{nl} \in \mathbb{C}^{M \times M}$ denotes the receive correlation matrix, and $\mathbf{h}_{nl}^{\text{iid}} \in \mathbb{C}^{M \times 1}$ denotes independent complex Gaussian matrix with zero mean and covariance matrix $\alpha_{nl} \mathbf{I}$. A ray-based 3D channel model from [34] is employed, and the receive correlation matrix \mathbf{R}_{nl} is approximated by

$$\mathbf{R}_{nl} \approx \mathbf{R}_{nl}^{\text{az}} \otimes \mathbf{R}_{nl}^{\text{el}}, \quad (2)$$

where $\mathbf{R}_{nl}^{\text{az}} \in \mathbb{R}^{W \times W}$ and $\mathbf{R}_{nl}^{\text{el}} \in \mathbb{R}^{D \times D}$ are the correlation matrices in azimuth and elevation directions, respectively, and are defined by [34]

$$[\mathbf{R}_{nl}^{\text{az}}]_{ww'} = \frac{1}{\sqrt{b}} \exp \left(-\frac{a^2 \cos^2(\theta_{nl}^{\text{az}}) - 2j c \cos(\theta_{nl}^{\text{az}}) + \nu_{nl}^{\text{az}} (c \sin(\theta_{nl}^{\text{az}}))^2}{2b} \right), \quad (3)$$

$$[\mathbf{R}_{nl}^{\text{el}}]_{dd'} = \exp \left(2 \frac{j \pi \lambda d^{\text{el}} (d' - d) \cos(\theta_{nl}^{\text{el}}) - \nu_{nl}^{\text{el}} (\pi d^{\text{el}} (d' - d) \sin(\theta_{nl}^{\text{el}}))^2}{\lambda^2} \right), \quad (4)$$

in terms of

$$a = \frac{2\pi d^{\text{az}}}{\lambda} \sqrt{\nu_{nl}^{\text{el}}} (w' - w) \cos(\theta_{nl}^{\text{el}}), \quad (5)$$

$$b = \nu_{nl}^{\text{az}} a^2 \sin^2(\theta_{nl}^{\text{az}}) + 1, \quad (6)$$

$$c = \frac{2\pi d_{\text{az}}}{\lambda} (w' - w) \sin(\theta_{nl}^{\text{el}}), \quad (7)$$

where λ is the carrier wavelength, θ_{nl}^{az} and θ_{nl}^{el} are the mean of horizontal angle-of-departure (AoD) and the mean of vertical AoD, respectively; ν_{nl}^{az} and ν_{nl}^{el} are the variance of horizontal AoD and the variance of vertical AoD, respectively; d_{el} and d_{az} are the vertical antenna spacing and the horizontal antenna spacing, respectively.

B. Signal Model

For the n th user, the information bits \mathbf{b}_n are encoded and interleaved, yielding a sequence of coded bits \mathbf{c}_n . Then each Q bits in \mathbf{c}_n are mapped to one modulation symbol \mathbf{x}_n^d , which is chosen from a 2^Q -ary constellation set \mathcal{A} , i.e., $|\mathcal{A}| = 2^Q$. The data symbols \mathbf{x}_n^d are then multiplexed with pilot symbols \mathbf{x}_n^p , forming the transmitted symbols sequence \mathbf{x}_n . Pilot and data symbols are arranged in an OFDM frame of T OFDM symbols, each consisting of K subcarriers. Specifically, the frequency-domain symbols in the t th OFDM symbols transmitted by the n th user are denoted by $\mathbf{x}_{tn} = [x_{tn1}, \dots, x_{tnK}]^T$, where $x_{tnk} \in \mathcal{A}$ denotes the symbol transmitted at the k th subcarrier. In each OFDM frame, there are $K_p \leq K$ pilot subcarriers in one selected OFDM symbol and the pilot subcarriers are spaced uniformly. The set of pilot-subcarriers of user n is denoted by $\mathcal{P}_n = \{(t, k) : x_{tnk} \text{ is a pilot symbol}\}$, $|\mathcal{P}_n| = K_p$, and the set of data-subcarriers is denoted by $\mathcal{D} = \overline{\bigcup_n \mathcal{P}_n}$. To maintain the orthogonality between the pilot sequences sent by different user, pilots symbols can be frequency division multiplexing, time division multiplexing, code division multiplexing or hybrid of them. For simplicity, the sets of pilot-subcarriers belong to different users are set to be mutually exclusive, i.e., $\bigcap_n \mathcal{P}_n = \emptyset$, and only one user actually transmits a pilot symbol at a given subcarrier, whereas the other users transmit zero-symbol at this subcarrier [35], i.e., $x_{tn'k} = 0, \forall n' \neq n$, if $(t, k) \in \mathcal{P}_n$. To modulate the OFDM symbol, a K -point inverse discrete Fourier transform (IDFT) is applied to the symbol sequence \mathbf{x}_{tn} and then a cyclic prefix (CP) is added before transmission.

At the receiver, the CP is removed first and then the received signal from each receive antenna is converted into frequency domain through a K -point discrete Fourier transform (DFT). It is assumed that the N transmitters and the receiver are synchronized and the duration of the cyclic prefix is larger than the maximum delays. And then the received signal during the interval of

the t th OFDM symbol can be written as

$$y_{tmk} = \sum_n w_{mnk} x_{tnk} + \varpi_{tmk}, \quad (8)$$

where y_{tmk} denotes the received signal at the k th subcarrier on the m th receive antenna, ϖ_{tmk} denotes a circularly symmetric complex noise with zero mean and the variance of σ_ϖ^2 , and w_{mnk} denotes the CFR at the k th subcarrier between the n th user and the m th receive antenna, which is given by

$$w_{mnk} = \sum_{l=1}^L h_{mnk} \exp\left(-\frac{j2\pi lk}{K}\right). \quad (9)$$

The received signal for a frame of T OFDM symbols can be recast in a matrix-vector form as

$$\mathbf{y} = \sum_{n=1}^N \mathbf{W}_n \mathbf{x}_n + \boldsymbol{\varpi} = \mathbf{W} \mathbf{x} + \boldsymbol{\varpi}, \quad (10)$$

where $\mathbf{y} = [\mathbf{y}_1^\top \cdots \mathbf{y}_M^\top]^\top$ with $\mathbf{y}_m = [y_{1m1} \cdots y_{1mK} \cdots y_{Tm1} \cdots y_{TmK}]^\top$ denoting the received signal at the m th receive antenna for T OFDM symbols, $\mathbf{W}_n = [\mathbf{I}_T \otimes \text{diag}\{\mathbf{w}_{1n}\} \cdots \mathbf{I}_T \otimes \text{diag}\{\mathbf{w}_{Mn}\}]^\top$ with $\mathbf{w}_{mn} = [w_{mn1} \cdots w_{mnK}]^\top$ denoting the CFR from the n th user to the m th antenna, $\mathbf{W} = [\mathbf{W}_1 \cdots \mathbf{W}_N]$, $\mathbf{x} = [\mathbf{x}_1^\top \cdots \mathbf{x}_N^\top]^\top$ with $\mathbf{x}_n = [x_{1n1} \cdots x_{1nK} \cdots x_{Tn1} \cdots x_{TnK}]^\top$ denoting the symbols transmitted by the n th user, and $\boldsymbol{\varpi} = [\boldsymbol{\varpi}_1^\top \cdots \boldsymbol{\varpi}_M^\top]^\top$ with $\boldsymbol{\varpi}_m = [\varpi_{1m1} \cdots \varpi_{1mK} \cdots \varpi_{Tm1} \cdots \varpi_{TmK}]^\top$ denoting the noise signal at the m th receive antenna.

C. Factor Graph Representation of the Massive MIMO-OFDM Systems

Our goal is to infer the information bits $\{\mathbf{b}_n\}$ from the observations \mathbf{y} with the known pilot symbols $\{\mathbf{x}_n^p\}$. In particular, we aim to achieve the minimum bit error rate (BER) utilizing the maximum *a posteriori* marginal criterion, i.e.,

$$\hat{b}_{n\iota} = \arg \max_{b_{n\iota} \in \{0,1\}} p(b_{n\iota} \mid \mathbf{y}), \quad (11)$$

where $b_{n\iota}$ denotes the ι th information bit in \mathbf{b}_n , and the *a posteriori* probability $p(b_{n\iota} \mid \mathbf{y})$ is given by

$$p(b_{n\iota} \mid \mathbf{y}) \propto \sum_{\mathbf{b} \setminus b_{n\iota}, \mathbf{c}, \mathbf{x}} \int_{\mathbf{H}, \mathbf{W}} p(\mathbf{b}, \mathbf{c}, \mathbf{x}, \mathbf{y}, \mathbf{W}, \mathbf{H}). \quad (12)$$

Since $\mathbf{b} \rightarrow \mathbf{c} \rightarrow \mathbf{x} \rightarrow \mathbf{y}$ is a Markov chain and the CFR matrix \mathbf{W} only depends on the CIR matrix \mathbf{H} , the joint probability $p(\mathbf{b}, \mathbf{c}, \mathbf{x}, \mathbf{y}, \mathbf{W}, \mathbf{H})$ can be factorized into

$$p(\mathbf{b}, \mathbf{c}, \mathbf{x}, \mathbf{y}, \mathbf{W}, \mathbf{H}) = p(\mathbf{b}) p(\mathbf{c} \mid \mathbf{b}) p(\mathbf{x} \mid \mathbf{c}) p(\mathbf{y} \mid \mathbf{W}, \mathbf{x}) p(\mathbf{H}, \mathbf{W}). \quad (13)$$

The conditional probability $p(\mathbf{x} \mid \mathbf{c})$ in (13) can be factorized into

$$p(\mathbf{x} \mid \mathbf{c}) = \prod_t p(\mathbf{x}_t \mid \mathbf{c}_t) = \prod_{t,n,k} p(x_{tnk} \mid \mathbf{c}_{tnk}), \quad (14)$$

where $\mathbf{c}_t \triangleq \{\mathbf{c}_{tnk}, \forall n, k\}$, $\mathbf{x}_t \triangleq \{x_{tnk}, \forall n, k\}$, $p(x_{tnk} \mid \mathbf{c}_{tnk}) = \delta(\varphi(\mathbf{c}_{tnk}) - x_{tnk})$ denotes the deterministic mapping $x_{tnk} = \varphi(\mathbf{c}_{tnk})$, $\varphi(\mathbf{c}_{tnk})$ is the mapping function and $\delta(\cdot)$ is the Kronecker delta function. In practice, the receive correlation matrices $\{\mathbf{R}_{nl}\}$ are unknown, so we impose a conditional independent structure on the *a priori* probability of \mathbf{H} , i.e.,

$$p(\mathbf{H} \mid \boldsymbol{\gamma}) = \prod_{n,l} p(\mathbf{h}_{\cdot nl} \mid \gamma_{nl}), \quad (15)$$

$$p(\mathbf{h}_{\cdot nl} \mid \gamma_{nl}) = \prod_m p(h_{mn} \mid \gamma_{nl}), \quad (16)$$

$$p(h_{mn} \mid \gamma_{nl}) = \mathcal{N}_{\mathbb{C}}(h_{mn}; \gamma_{nl}^{-1}), \quad (17)$$

$$p(\gamma_{nl}) = \text{Gam}(\gamma_{nl}; 0, 0), \quad (18)$$

where $\boldsymbol{\gamma} \triangleq \{\gamma_{nl}\}$, and γ_{nl} is the inversion of PDP to be learned. As the CFR \mathbf{w}_{mn} is the Fourier transformations of the CIR \mathbf{h}_{mn} , i.e., $\mathbf{w}_{mn} = \boldsymbol{\Phi} \mathbf{h}_{mn}, \forall m, \forall n$, then the conditional probability $p(\mathbf{W} \mid \mathbf{H})$ reads

$$p(\mathbf{W} \mid \mathbf{H}) = \prod_{m,n} p(\mathbf{w}_{mn} \mid \mathbf{h}_{mn}) = \prod_{m,n,k} \delta\left(w_{mnk} - \sum_l \phi_{kl} h_{mn}^l\right), \quad (19)$$

where $\boldsymbol{\Phi} \in \mathbb{C}^{K \times L}$ denotes the DFT weighting matrix, and ϕ_{kl} denotes the entry in the k th row and l th column of $\boldsymbol{\Phi}$. The channel transition function $p(\mathbf{y} \mid \mathbf{W}, \mathbf{x})$ is factorized into

$$p(\mathbf{y} \mid \mathbf{W}, \mathbf{x}) = \prod_{t,m,k} f_{tmk}(\mathbf{x}_{t \cdot k}, \mathbf{w}_{m \cdot k}), \quad (20)$$

where $\mathbf{x}_{t \cdot k} \triangleq [x_{t1k} \cdots x_{tNk}]^T$, $\mathbf{w}_{m \cdot k} \triangleq [w_{m1k} \cdots w_{mNk}]^T$, and

$$f_{tmk}(\mathbf{x}_{t \cdot k}, \mathbf{w}_{m \cdot k}) = \mathcal{N}_{\mathbb{C}}\left(y_{tmk}; \sum_n w_{mnk} x_{mnk}, \sigma_{\varpi}^2\right). \quad (21)$$

The probabilistic structure defined by the factorizations (13)-(20) can be represented by the factor graph, as depicted in Fig. 1. In this factor graph, mapping constraint $\delta(\varphi(\mathbf{c}_{tnk}) - x_{tnk})$ appears as a function node \mathcal{M}_{tnk} , the mixing constraint $\delta(w_{mnk} - \sum_l \phi_{kl} h_{mn}^l)$ appears as function node g_{mnk} , and the *a priori* distribution $\psi(h_{mn}, \gamma_{nl})$ appears as function node ψ_{mn} .

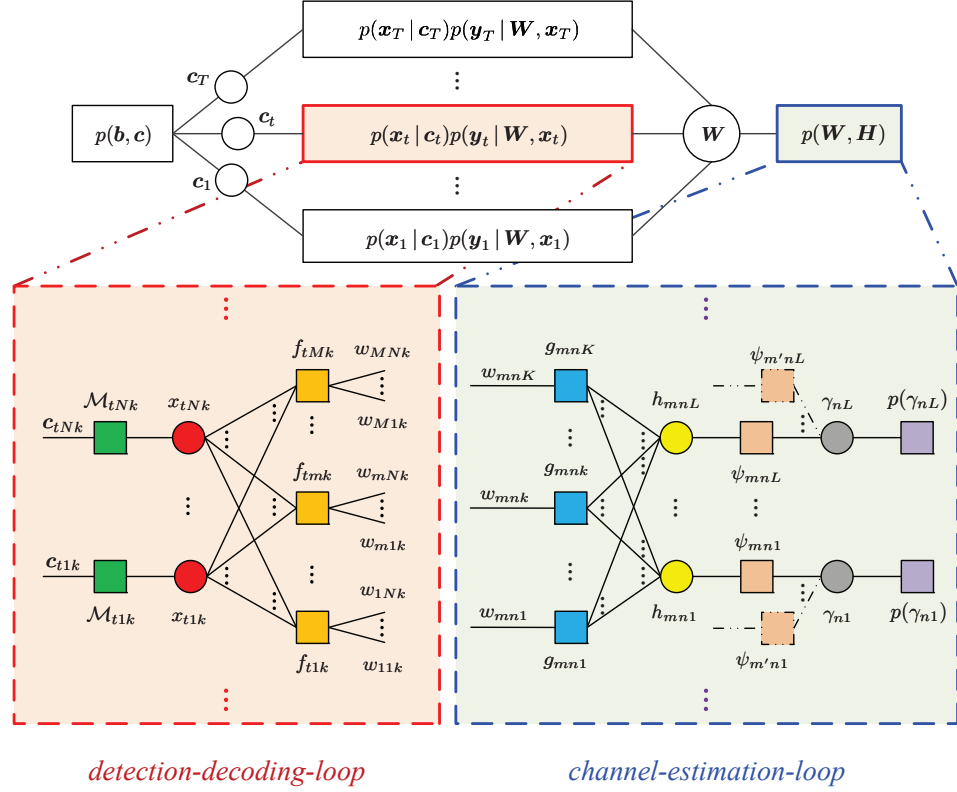


Figure 1: Factor graph of the massive MIMO-OFDM system.

There exist two groups of loops, the *detection-decoding-loop* on the left and the *channel-estimation-loop* on the right. Unlike a tree-structured factor graph, the existence of loops implies various iterative message passing schedules. In our case, we choose to start passing messages at the channel transition nodes $\{f_{tmk}\}$, then pass messages concurrently in both the *detection-decoding-loop* and the *channel-estimation-loop*. Each of these full cycles of message passing will be referred to as a “turbo iteration”.

III. EXPECTATION PROPAGATION FOR JOINT CHANNEL ESTIMATION AND DECODING

The presentation of message passing follows closely with the convention in [13]. Due to high-dimensional integration, directly applying the SPA to the factor graph in Fig. 1 is computationally prohibitive. Hence, we resort to approximate inference to find efficient solutions.

A. Message Updating in Detection-Decoding-Loop

Note that, to update the outgoing messages from the channel transition node f_{tmk} , the received signal shown in (8) can be rewritten as

$$y_{tmk} = w_{mnk}x_{tnk} + \sum_{n' \neq n} w_{mn'k}x_{tn'k} + \varpi_{tmk}, \forall n. \quad (22)$$

The interference term $\sum_{n' \neq n} w_{mn'k}x_{tn'k} + \varpi_{tmk}$ in (22) is considered as a Gaussian variable [32], [36], and then $y_{tmk} - (\sum_{n' \neq n} w_{mn'k}x_{tn'k} + \varpi_{tmk})$ is also a Gaussian variable with the mean $z_{f_{tmk} \rightarrow x_{tnk}}^{(i)}$ and variance $\tau_{f_{tmk} \rightarrow x_{tnk}}^{(i)}$ given by

$$z_{f_{tmk} \rightarrow x_{tnk}}^{(i)} = y_{tmk} - \sum_{n' \neq n} \hat{w}_{w_{mn'k} \rightarrow f_{tmk}}^{(i-1)} \hat{x}_{x_{tn'k} \rightarrow f_{tmk}}^{(i-1)}, \quad (23)$$

$$\begin{aligned} \tau_{f_{tmk} \rightarrow x_{tnk}}^{(i)} = \sigma_{\varpi}^2 + \sum_{n' \neq n} & \left(\left| \hat{w}_{w_{mn'k} \rightarrow f_{tmk}}^{(i-1)} \right|^2 \nu_{x_{tn'k} \rightarrow f_{tmk}}^{(i-1)} \right. \\ & \left. + \nu_{w_{mn'k} \rightarrow f_{tmk}}^{(i-1)} \left| \hat{x}_{x_{tn'k} \rightarrow f_{tmk}}^{(i-1)} \right|^2 + \nu_{w_{mn'k} \rightarrow f_{tmk}}^{(i-1)} \nu_{x_{tn'k} \rightarrow f_{tmk}}^{(i-1)} \right), \end{aligned} \quad (24)$$

where $\hat{x}_{x_{tnk} \rightarrow f_{tmk}}^{(i-1)}$ and $\nu_{x_{tnk} \rightarrow f_{tmk}}^{(i-1)}$ denote the mean and variance of variable x_{tnk} with respect to the message $\mu_{x_{tnk} \rightarrow f_{tmk}}^{(i-1)}(x_{tnk})$; $\hat{w}_{w_{mnk} \rightarrow f_{tmk}}^{(i-1)}$ and $\nu_{w_{mnk} \rightarrow f_{tmk}}^{(i-1)}$ denote the mean and variance of variable w_{mnk} with respect to the message $\mu_{w_{mnk} \rightarrow f_{tmk}}^{(i-1)}(w_{mnk})$. From the model shown in (22)-(24), the channel transition function f_{tmk} at the i th turbo iteration can be viewed as

$$\hat{f}_{tmk}^{(i)}(w_{mnk}, x_{tnk}) = \mathcal{N}_{\mathbb{C}} \left(w_{mnk}x_{tnk}; z_{f_{tmk} \rightarrow x_{tnk}}^{(i)}, \tau_{f_{tmk} \rightarrow x_{tnk}}^{(i)} \right), \forall n \quad (25)$$

Consequently, the message $\mu_{f_{tmk} \rightarrow x_{tnk}}^{(i)}(x_{tnk})$ is calculated by

$$\begin{aligned} \mu_{f_{tmk} \rightarrow x_{tnk}}^{(i)}(x_{tnk}) &= \int_{w_{mnk}} \hat{f}_{tmk}^{(i)}(w_{mnk}, x_{tnk}) \mu_{w_{mnk} \rightarrow f_{tmk}}^{(i-1)}(w_{mnk}) \\ &\propto \mathcal{N}_{\mathbb{C}} \left(x_{tnk}; \frac{z_{f_{tmk} \rightarrow x_{tnk}}^{(i)} - \hat{w}_{w_{mnk} \rightarrow f_{tmk}}^{(i-1)} x_{tnk}}{\left| \hat{w}_{w_{mnk} \rightarrow f_{tmk}}^{(i-1)} \right|^2}, \frac{\tau_{f_{tmk} \rightarrow x_{tnk}}^{(i)} + \nu_{w_{mnk} \rightarrow f_{tmk}}^{(i-1)} |x_{tnk}|^2}{\left| \hat{w}_{w_{mnk} \rightarrow f_{tmk}}^{(i-1)} \right|^2} \right). \end{aligned} \quad (26)$$

Using (26), the message from the variable x_{tnk} to the channel transition node f_{tmk} is updated by

$$\mu_{x_{tnk} \rightarrow f_{tmk}}^{(i)}(x_{tnk}) = \mu_{\mathcal{M}_{tnk} \rightarrow x_{tnk}}^{(i)}(x_{tnk}) \exp \left(- \sum_{m' \neq m} \Delta_{f_{tm'k} \rightarrow x_{tnk}}^{(i)}(x_{tnk}) \right), \quad (27)$$

where

$$\Delta_{f_{tmk} \rightarrow x_{tnk}}^{(i)}(x_{tnk}) = \frac{\left| z_{f_{tmk} \rightarrow x_{tnk}}^{(i)} - \hat{w}_{w_{mnk} \rightarrow f_{tmk}}^{(i-1)} x_{tnk} \right|^2}{\tau_{f_{tmk} \rightarrow x_{tnk}}^{(i)} + \nu_{w_{mnk} \rightarrow f_{tmk}}^{(i-1)} |x_{tnk}|^2} + \ln \left(\tau_{f_{tmk} \rightarrow x_{tnk}}^{(i)} + \nu_{w_{mnk} \rightarrow f_{tmk}}^{(i-1)} |x_{tnk}|^2 \right). \quad (28)$$

To obtain $z_{f_{tmk} \rightarrow x_{tnk}}^{(i)}$ in (23) and $\tau_{f_{tmk} \rightarrow x_{tnk}}^{(i)}$ in (24), the mean and variance of variable x_{tnk} with respect to the message $\mu_{x_{tnk} \rightarrow f_{tmk}}^{(i-1)}(x_{tnk})$ are calculated by

$$\hat{x}_{x_{tnk} \rightarrow f_{tmk}}^{(i-1)} = \frac{\sum_{\alpha_s \in \mathcal{A}} \alpha_s \mu_{x_{tnk} \rightarrow f_{tmk}}^{(i-1)}(x_{tnk} = \alpha_s)}{\sum_{\alpha_s \in \mathcal{A}} \mu_{x_{tnk} \rightarrow f_{tmk}}^{(i-1)}(x_{tnk} = \alpha_s)}, \quad (29)$$

$$\nu_{x_{tnk} \rightarrow f_{tmk}}^{(i-1)} = \frac{\sum_{\alpha_s \in \mathcal{A}} |\alpha_s|^2 \mu_{x_{tnk} \rightarrow f_{tmk}}^{(i-1)}(x_{tnk} = \alpha_s)}{\sum_{\alpha_s \in \mathcal{A}} \mu_{x_{tnk} \rightarrow f_{tmk}}^{(i-1)}(x_{tnk} = \alpha_s)} - |\hat{x}_{x_{tnk} \rightarrow f_{tmk}}^{(i-1)}|^2. \quad (30)$$

Using the Gaussian approximation shown in (22)-(24) again, the message $\mu_{f_{tmk} \rightarrow w_{mnk}}^{(i)}(w_{mnk})$ is then updated by

$$\mu_{f_{tmk} \rightarrow w_{mnk}}^{(i)}(w_{mnk}) \propto \sum_{x_{tnk} \in \mathcal{A}} \vartheta_{f_{tmk}}^{(i)}(x_{tnk}) \mathcal{N}_{\mathbb{C}} \left(w_{mnk}; \frac{z_{f_{tmk} \rightarrow x_{tnk}}^{(i)}}{x_{tnk}}, \frac{\tau_{f_{tmk} \rightarrow x_{tnk}}^{(i)}}{|x_{tnk}|^2} \right), \quad (31)$$

where $\vartheta_{f_{tmk}}^{(i)}(x_{tnk})$ denotes the weight of Gaussian component,

$$\vartheta_{f_{tmk}}^{(i)}(x_{tnk}) = \frac{|x_{tnk}|^{-2} \mu_{x_{tnk} \rightarrow f_{tmk}}^{(i-1)}(x_{tnk})}{\sum_{x_{tnk} \in \mathcal{A}} |x_{tnk}|^{-2} \mu_{x_{tnk} \rightarrow f_{tmk}}^{(i-1)}(x_{tnk})}, x_{tnk} \in \mathcal{A}. \quad (32)$$

As $\mu_{f_{tmk} \rightarrow w_{mnk}}^{(i)}(w_{mnk})$ given by (31) is a Gaussian mixture, the number of its components will increase exponentially in the consequent message updating. To avoid the increase, the message $\mu_{f_{tmk} \rightarrow w_{mnk}}^{(i)}(w_{mnk})$ can be projected onto a Gaussian function by the criterion of minimum KL divergence as in [8] and [16]. The projection reduces to matching the first two order moments of a Gaussian function $\mathcal{N}_{\mathbb{C}}(w_{mnk}; \hat{w}_{f_{tmk} \rightarrow w_{mnk}}^{(i)}, \nu_{f_{tmk} \rightarrow w_{mnk}}^{(i)})$ and the message $\mu_{f_{tmk} \rightarrow w_{mnk}}^{(i)}(w_{mnk})$ [37], leading to

$$\hat{w}_{f_{tmk} \rightarrow w_{mnk}}^{(i)} = z_{f_{tmk} \rightarrow x_{tnk}}^{(i)} \sum_{x_{tnk} \in \mathcal{A}} \frac{\vartheta_{f_{tmk}}^{(i)}(x_{tnk})}{x_{tnk}}, \quad (33)$$

$$\nu_{f_{tmk} \rightarrow w_{mnk}}^{(i)} = \left(\tau_{f_{tmk} \rightarrow x_{tnk}}^{(i)} + \left| z_{f_{tmk} \rightarrow x_{tnk}}^{(i)} \right|^2 \right) \sum_{x_{tnk} \in \mathcal{A}} \frac{\vartheta_{f_{tmk}}^{(i)}(x_{tnk})}{|x_{tnk}|^2} - \left| \hat{w}_{f_{tmk} \rightarrow w_{mnk}}^{(i)} \right|^2. \quad (34)$$

The Gaussian approximations shown in (22)-(34) lead to a desirable closed-form message passing algorithm, which will be referred to as “BP-GA”. However, it bears a heavy computations burden: it needs to calculate each $\mu_{x_{tnk} \rightarrow f_{tmk}}^{(i)}(x_{tnk}), \forall x_{tnk} \in \mathcal{A}$, but the term $-\sum_{m' \neq m} \Delta_{f_{tm'k} \rightarrow x_{tnk}}^{(i)}(x_{tnk})$ in (27) is complex as M is large in the massive MIMO systems. Besides, it needs to calculate each $\hat{x}_{x_{tnk} \rightarrow f_{tmk}}^{(i-1)}$ and $\nu_{x_{tnk} \rightarrow f_{tmk}}^{(i-1)}$ using (29) and (30), which amounts to $TMNK$.

Next, we will derive an efficient message-passing algorithm by the framework of expectation propagation. Recalling (22)-(24), a local belief of w_{mnk} at the channel-transition function f_{tnk} can be defined by

$$\begin{aligned}\beta_{f_{tnk}}^{(i)}(w_{mnk}) &= \mu_{w_{mnk} \rightarrow f_{tnk}}^{(i-1)}(w_{mnk}) \int_{x_{tnk}} \hat{f}_{tnk}^{(i)}(w_{mnk}, x_{tnk}) \mu_{x_{tnk} \rightarrow f_{tnk}}^{(i-1)}(x_{tnk}) \\ &\propto \exp\left(-\Delta_{f_{tnk}}^{(i)}(w_{mnk})\right), \forall n,\end{aligned}\quad (35)$$

where

$$\begin{aligned}\Delta_{f_{tnk}}^{(i)}(w_{mnk}) &= \frac{\left|z_{f_{tnk} \rightarrow x_{tnk}}^{(i)} - \hat{x}_{x_{tnk} \rightarrow f_{tnk}}^{(i-1)} w_{mnk}\right|^2}{\tau_{f_{tnk} \rightarrow x_{tnk}}^{(i)} + \nu_{x_{tnk} \rightarrow f_{tnk}}^{(i-1)} |w_{mnk}|^2} + \frac{\left|w_{mnk} - w_{w_{mnk} \rightarrow f_{tnk}}^{(i-1)}\right|^2}{\nu_{w_{mnk} \rightarrow f_{tnk}}^{(i-1)}} \\ &\quad + \ln\left(\tau_{f_{tnk} \rightarrow x_{tnk}}^{(i)} + \nu_{x_{tnk} \rightarrow f_{tnk}}^{(i-1)} |w_{mnk}|^2\right).\end{aligned}\quad (36)$$

We impose a continuous complex Gaussian distribution constraint on the belief of w_{mnk} , i.e., we project $\beta_{f_{tnk}}^{(i)}(w_{mnk})$ to a Gaussian distribution. The projection reduces to a moment matching; however, the mean and variance of $\beta_{f_{tnk}}^{(i)}(w_{mnk})$ involve complex integrals and there are no analytical solutions. So we resort to quadratic approximation for calculating the first two moments of $\beta_{f_{tnk}}^{(i)}(w_{mnk})$.

The term $z_{f_{tnk} \rightarrow x_{tnk}}^{(i)} - \hat{x}_{x_{tnk} \rightarrow f_{tnk}}^{(i-1)} w_{mnk}$, $\tau_{f_{tnk} \rightarrow x_{tnk}}^{(i)} + \nu_{x_{tnk} \rightarrow f_{tnk}}^{(i-1)} |w_{mnk}|^2$, and $w_{mnk} - w_{w_{mnk} \rightarrow f_{tnk}}^{(i-1)}$ in (36) can be rewritten as

$$\begin{aligned}z_{f_{tnk} \rightarrow x_{tnk}}^{(i)} - \hat{x}_{x_{tnk} \rightarrow f_{tnk}}^{(i-1)} w_{mnk} &= \underbrace{z_{f_{tnk} \rightarrow x_{tnk}}^{(i)} - \hat{x}_{x_{tnk} \rightarrow f_{tnk}}^{(i-1)} \hat{w}_{w_{mnk}}^{(i-1)}}_{\hat{z}_{f_{tnk} \rightarrow w_{mnk}}^{(i)}} \\ &\quad + \hat{x}_{x_{tnk} \rightarrow f_{tnk}}^{(i-1)} (\hat{w}_{w_{mnk}}^{(i-1)} - w_{mnk}),\end{aligned}\quad (37)$$

$$\begin{aligned}\tau_{f_{tnk} \rightarrow x_{tnk}}^{(i)} + \nu_{x_{tnk} \rightarrow f_{tnk}}^{(i-1)} |w_{mnk}|^2 &= \underbrace{\tau_{f_{tnk} \rightarrow x_{tnk}}^{(i)} + \nu_{x_{tnk} \rightarrow f_{tnk}}^{(i-1)} |\hat{w}_{w_{mnk}}^{(i-1)}|^2}_{\hat{\tau}_{f_{tnk} \rightarrow w_{mnk}}^{(i)}} \\ &\quad + \nu_{x_{tnk} \rightarrow f_{tnk}}^{(i-1)} \left(|w_{mnk}|^2 - |\hat{w}_{w_{mnk}}^{(i-1)}|^2\right),\end{aligned}\quad (38)$$

$$w_{mnk} - \hat{w}_{w_{mnk} \rightarrow f_{tnk}}^{(i-1)} = \hat{w}_{w_{mnk}}^{(i-1)} - \hat{w}_{w_{mnk} \rightarrow f_{tnk}}^{(i-1)} + (w_{mnk} - \hat{w}_{w_{mnk}}^{(i-1)}). \quad (39)$$

where $\hat{w}_{w_{mnk}}^{(i-1)}$ is the *a posteriori* mean of w_{mnk} at previous turbo iteration. By (76) shown in the Appendix, we can expand $\Delta_{f_{tnk}}^{(i)}(x_{tnk})$ at the point $\vec{z}_0 = [\hat{z}_{f_{tnk} \rightarrow w_{mnk}}^{(i)}, (\hat{z}_{f_{tnk} \rightarrow w_{mnk}}^{(i)})^*]$,

$$\tau_0 = \hat{\tau}_{f_{tmk} \rightarrow w_{mnk}}^{(i)}, \text{ and } \vec{u}_0 = [\hat{w}_{w_{mnk}}^{(i-1)} - \hat{w}_{w_{mnk} \rightarrow f_{tmk}}^{(i-1)}, (\hat{w}_{w_{mnk}}^{(i-1)} - \hat{w}_{w_{mnk} \rightarrow f_{tmk}}^{(i-1)})^*], \text{ i.e.,}$$

$$\Delta_{f_{mnk}}^{(i)}(w_{mnk}) = \left(\frac{1}{\nu_{w_{mnk} \rightarrow f_{tmk}}^{(i-1)}} + \frac{|\hat{x}_{x_{tnk} \rightarrow f_{tmk}}^{(i-1)}|^2}{\hat{\tau}_{f_{tmk} \rightarrow w_{mnk}}^{(i)}} + \frac{\nu_{x_{tnk} \rightarrow f_{tmk}}^{(i-1)} \left(1 - \frac{|\hat{z}_{f_{tmk} \rightarrow w_{mnk}}^{(i)}|^2}{\hat{\tau}_{f_{tmk} \rightarrow w_{mnk}}^{(i)}} \right)}{\hat{\tau}_{f_{tmk} \rightarrow w_{mnk}}^{(i)}} \right) |w_{mnk}|^2$$

$$- 2\Re \left\{ \frac{(\hat{z}_{f_{tmk} \rightarrow x_{tnk}}^{(i)})^* \hat{x}_{x_{tnk} \rightarrow f_{tmk}}^{(i-1)}}{\hat{\tau}_{f_{tmk} \rightarrow w_{mnk}}^{(i)}} w_{mnk} + \frac{(\hat{w}_{w_{mnk} \rightarrow f_{tmk}}^{(i-1)})^*}{\nu_{w_{mnk} \rightarrow f_{tmk}}^{(i-1)}} w_{mnk} \right\} + \text{const}, \quad (40)$$

where the invariant terms with respect to w_{mnk} are absorbed into the constant term const . Note that using (40) $\exp\{-\Delta_{f_{mnk}}^{(i)}(w_{mnk})\}$ is essentially the Gaussian approximation of $\beta_{f_{tmk}}^{(i)}(w_{mnk})$, i.e.,

$$\beta_{f_{tmk}}^{(i)}(w_{mnk}) \approx \mathcal{N}_{\mathbb{C}} \left(w_{mnk}; \hat{w}_{f_{tmk}}^{(i)}, \nu_{f_{tmk}}^{(i)} \right), \quad (41)$$

where

$$\nu_{f_{tmk}}^{(i)} = \frac{\hat{\tau}_{f_{tmk} \rightarrow w_{mnk}}^{(i)}}{\frac{\hat{\tau}_{f_{tmk} \rightarrow w_{mnk}}^{(i)}}{\nu_{w_{mnk} \rightarrow f_{tmk}}^{(i-1)}} + |\hat{x}_{x_{tnk} \rightarrow f_{tmk}}^{(i-1)}|^2 + \nu_{x_{tnk} \rightarrow f_{tmk}}^{(i-1)} \left(1 - \frac{|\hat{z}_{f_{tmk} \rightarrow w_{mnk}}^{(i)}|^2}{\hat{\tau}_{f_{tmk} \rightarrow w_{mnk}}^{(i)}} \right)}, \quad (42)$$

$$\hat{w}_{f_{tmk}}^{(i)} = \nu_{f_{tmk}}^{(i)} \left(\frac{(\hat{x}_{x_{tnk} \rightarrow f_{tmk}}^{(i-1)})^* \hat{z}_{f_{tmk} \rightarrow x_{tnk}}^{(i)}}{\hat{\tau}_{f_{tmk} \rightarrow w_{mnk}}^{(i)}} + \frac{\hat{w}_{w_{mnk} \rightarrow f_{tmk}}^{(i-1)}}{\nu_{w_{mnk} \rightarrow f_{tmk}}^{(i-1)}} \right). \quad (43)$$

Using the expectation propagation principle and (41), we get

$$\mu_{f_{tmk} \rightarrow w_{mnk}}^{(i)} = \frac{\beta_{f_{tmk}}^{(i)}(w_{mnk})}{\mu_{w_{mnk} \rightarrow f_{tmk}}^{(i-1)}} \propto \mathcal{N}_{\mathbb{C}} \left(w_{mnk}; \hat{w}_{f_{tmk} \rightarrow w_{mnk}}^{(i)}, \nu_{f_{tmk} \rightarrow w_{mnk}}^{(i)} \right), \quad (44)$$

where

$$\nu_{f_{tmk} \rightarrow w_{mnk}}^{(i)} = \frac{\hat{\tau}_{f_{tmk} \rightarrow w_{mnk}}^{(i)}}{|\hat{x}_{x_{tnk} \rightarrow f_{tmk}}^{(i-1)}|^2 + \nu_{x_{tnk} \rightarrow f_{tmk}}^{(i-1)} \left(1 - \frac{|\hat{z}_{f_{tmk} \rightarrow w_{mnk}}^{(i)}|^2}{\hat{\tau}_{f_{tmk} \rightarrow w_{mnk}}^{(i)}} \right)}, \quad (45)$$

$$\hat{w}_{f_{tmk} \rightarrow w_{mnk}}^{(i)} = \nu_{f_{tmk} \rightarrow w_{mnk}}^{(i)} \frac{(\hat{x}_{x_{tnk} \rightarrow f_{tmk}}^{(i-1)})^* \hat{z}_{f_{tmk} \rightarrow x_{tnk}}^{(i)}}{\hat{\tau}_{f_{tmk} \rightarrow w_{mnk}}^{(i)}}. \quad (46)$$

Note that, the messages at the channel transition nodes associated with known pilot symbol boil down to the following simple form

$$\mu_{f_{tmk} \rightarrow w_{mnk}}^{(i)}(w_{mnk}) \propto \mathcal{N}_{\mathbb{C}} \left(w_{mnk}; \frac{y_{tnk}}{|x_{tnk}|^2}, \frac{\sigma_{\varpi}^2}{|x_{tnk}|^2} \right), \forall (t, k) \in \mathcal{P}_n, \quad (47)$$

where we use the fact that other users transmit zero-symbols on the pilot subcarriers \mathcal{P}_n , and pilot symbol x_{tnk} takes a known value.

Similarly, at the channel-transition function f_{tnk} , a local belief of x_{tnk} can be defined by

$$\beta_{f_{tnk}}^{(i)}(x_{tnk}) \propto \exp\left(-\Delta_{f_{tnk}}^{(i)}(x_{tnk})\right), \quad (48)$$

where

$$\Delta_{f_{tnk}}^{(i)}(x_{tnk}) = \Delta_{f_{tnk} \rightarrow x_{tnk}}^{(i)}(x_{tnk}) + \frac{|x_{tnk} - \hat{x}_{x_{tnk} \rightarrow f_{tnk}}^{(i-1)}|^2}{\nu_{x_{tnk} \rightarrow f_{tnk}}^{(i-1)}}. \quad (49)$$

The term $z_{f_{tnk} \rightarrow x_{tnk}}^{(i)} - \hat{w}_{w_{mnk} \rightarrow f_{tnk}}^{(i-1)} x_{tnk}$, $\tau_{f_{tnk} \rightarrow x_{tnk}}^{(i)} + \nu_{w_{mnk} \rightarrow f_{tnk}}^{(i-1)} |x_{tnk}|^2$ and $x_{tnk} - \hat{x}_{x_{tnk} \rightarrow f_{tnk}}^{(i-1)}$ in (49) can also be rewritten as

$$\begin{aligned} z_{f_{tnk} \rightarrow x_{tnk}}^{(i)} - \hat{w}_{w_{mnk} \rightarrow f_{tnk}}^{(i-1)} x_{tnk} &= \underbrace{z_{f_{tnk} \rightarrow x_{tnk}}^{(i)} - \hat{w}_{w_{mnk} \rightarrow f_{tnk}}^{(i-1)} \hat{x}_{x_{tnk}}^{(i-1)}}_{\hat{z}_{f_{tnk} \rightarrow x_{tnk}}^{(i)}} \\ &\quad + \hat{w}_{w_{mnk} \rightarrow f_{tnk}}^{(i-1)} (\hat{x}_{x_{tnk}}^{(i-1)} - x_{tnk}), \end{aligned} \quad (50)$$

$$\begin{aligned} \tau_{f_{tnk} \rightarrow x_{tnk}}^{(i)} + \nu_{w_{mnk} \rightarrow f_{tnk}}^{(i-1)} |x_{tnk}|^2 &= \underbrace{\tau_{f_{tnk} \rightarrow x_{tnk}}^{(i)} + \nu_{w_{mnk} \rightarrow f_{tnk}}^{(i-1)} |\hat{x}_{x_{tnk}}^{(i-1)}|^2}_{\hat{\tau}_{f_{tnk} \rightarrow x_{tnk}}^{(i)}} \\ &\quad + \nu_{w_{mnk} \rightarrow f_{tnk}}^{(i-1)} (|x_{tnk}|^2 - |\hat{x}_{x_{tnk}}^{(i-1)}|^2), \end{aligned} \quad (51)$$

$$x_{tnk} - \hat{x}_{x_{tnk} \rightarrow f_{tnk}}^{(i-1)} = \hat{x}_{x_{tnk}}^{(i-1)} - \hat{x}_{x_{tnk} \rightarrow f_{tnk}}^{(i-1)} + (x_{tnk} - \hat{x}_{x_{tnk}}^{(i-1)}), \quad (52)$$

where $\hat{x}_{x_{tnk}}^{(i-1)}$ is the *a posteriori* mean of x_{tnk} at previous turbo iteration. Then $\Delta_{f_{tnk}}^{(i)}(x_{tnk})$ is expanded at the point at the point $\vec{z}_0 = [\hat{z}_{f_{tnk} \rightarrow x_{tnk}}^{(i)}, (\hat{z}_{f_{tnk} \rightarrow x_{tnk}}^{(i)})^*]$, $\tau_0 = \hat{\tau}_{f_{tnk} \rightarrow x_{tnk}}^{(i)}$, and $\vec{u}_0 = [\hat{x}_{x_{tnk}}^{(i-1)} - \hat{x}_{x_{tnk} \rightarrow f_{tnk}}^{(i-1)}, (\hat{x}_{x_{tnk}}^{(i-1)} - \hat{x}_{x_{tnk} \rightarrow f_{tnk}}^{(i-1)})^*]$, and we have

$$\mu_{f_{tnk} \rightarrow x_{tnk}}^{(i)}(x_{tnk}) \propto \mathcal{N}_{\mathbb{C}}\left(x_{tnk}; \hat{x}_{f_{tnk} \rightarrow x_{tnk}}^{(i)}, \nu_{f_{tnk} \rightarrow x_{tnk}}^{(i)}\right), \quad (53)$$

where $\hat{x}_{f_{tnk} \rightarrow x_{tnk}}^{(i)}$ and $\nu_{f_{tnk} \rightarrow x_{tnk}}^{(i)}$ are given by

$$\nu_{f_{tnk} \rightarrow x_{tnk}}^{(i)} = \frac{\hat{\tau}_{f_{tnk} \rightarrow x_{tnk}}^{(i)}}{|\hat{w}_{w_{mnk} \rightarrow f_{tnk}}^{(i-1)}|^2 + \nu_{w_{mnk} \rightarrow f_{tnk}}^{(i-1)} \left(1 - \frac{|\hat{z}_{f_{tnk} \rightarrow x_{tnk}}^{(i)}|^2}{\hat{\tau}_{f_{tnk} \rightarrow x_{tnk}}^{(i)}}\right)}, \quad (54)$$

$$\hat{x}_{f_{tnk} \rightarrow x_{tnk}}^{(i)} = \nu_{f_{tnk} \rightarrow x_{tnk}}^{(i)} \frac{(\hat{w}_{w_{mnk} \rightarrow f_{tnk}}^{(i-1)})^* \hat{z}_{f_{tnk} \rightarrow x_{tnk}}^{(i)}}{\hat{\tau}_{f_{tnk} \rightarrow x_{tnk}}^{(i)}}. \quad (55)$$

The message $\mu_{x_{tnk} \rightarrow \mathcal{M}_{tnk}}^{(i)}(x_{tnk})$ from the variable node x_{tnk} to the mapper node \mathcal{M}_{tnk} is updated by

$$\mu_{x_{tnk} \rightarrow \mathcal{M}_{tnk}}^{(i)}(x_{tnk}) = \prod_m \mu_{f_{tnk} \rightarrow x_{tnk}}^{(i)}(x_{tnk}) \propto \mathcal{N}_{\mathbb{C}}\left(x_{tnk}; \zeta_{x_{tnk}}^{(i)}, \gamma_{x_{tnk}}^{(i)}\right), \quad (56)$$

where $\gamma_{x_{tnk}}^{(i)} = 1 / \sum_m (1 / \nu_{f_{tnk} \rightarrow x_{tnk}}^{(i)})$ and $\zeta_{x_{tnk}}^{(i)} = \gamma_{x_{tnk}}^{(i)} \sum_m (\hat{x}_{f_{tnk} \rightarrow x_{tnk}}^{(i)} / \nu_{f_{tnk} \rightarrow x_{tnk}}^{(i)})$. With the message $\mu_{x_{tnk} \rightarrow \mathcal{M}_{tnk}}^{(i)}(x_{tnk}^k)$ and the *a priori* LLRs $\{\lambda_a^{(i)}(c_{tnk}^q), \forall q\}$ fed back by the decoder of user n at the previous turbo iteration, the extrinsic LLRs $\{\lambda_e^{(i)}(c_{tnk}^q), \forall q\}$ corresponding to the symbol x_{tnk} are mapped by

$$\lambda_e^{(i)}(c_{tnk}^q) = \ln \frac{\sum_{x_{tnk} \in \mathcal{A}_q^1} \mu_{x_{tnk} \rightarrow \mathcal{M}_{tnk}}^{(i)}(x_{tnk}) \mu_{\mathcal{M}_{tnk} \rightarrow x_{tnk}}^{(i-1)}(x_{tnk})}{\sum_{x_{tnk} \in \mathcal{A}_q^0} \mu_{x_{tnk} \rightarrow \mathcal{M}_{tnk}}^{(i)}(x_{tnk}) \mu_{\mathcal{M}_{tnk} \rightarrow x_{tnk}}^{(i-1)}(x_{tnk})} - \lambda_a^{(i-1)}(c_{tnk}^q), \quad (57)$$

where the $(i-1)$ th message $\mu_{\mathcal{M}_{tnk} \rightarrow x_{tnk}}^{(i-1)}(x_{tnk})$ is given in the following by (58). Once the extrinsic LLRs $\{\lambda_e^{(i)}(c_{tnk}^q)\}$ are available, each channel decoder performs decoding and feeds back the *a priori* LLRs of coded bits $\{\lambda_a^{(i)}(c_{tnk}^q)\}$, which then are interleaved and converted to the following message

$$\mu_{\mathcal{M}_{tnk} \rightarrow x_{tnk}}^{(i)}(x_{tnk}) = \prod_q \frac{\exp\left(c_{tnk}^q \cdot \lambda_a^{(i)}(c_{tnk}^q)\right)}{1 + \exp\left(\lambda_a^{(i)}(c_{tnk}^q)\right)}. \quad (58)$$

At the variable nodes $\{x_{tnk}\}$, the number of message parameters $\{\hat{x}_{x_{tnk} \rightarrow f_{tnk}}^{(i)}, \nu_{x_{tnk} \rightarrow f_{tnk}}^{(i)}\}$ reaches up to $2TMNK$, so directly evaluating them is expensive via moment matching like (29) and (30). Following the expectation propagation method, we can reduce the computational complexity of $\{\hat{x}_{x_{tnk} \rightarrow f_{tnk}}^{(i)}, \nu_{x_{tnk} \rightarrow f_{tnk}}^{(i)}\}$. First, at the variable node x_{tnk} , the local belief of x_{tnk} is defined by

$$\beta_{x_{tnk}}^{(i)}(x_{tnk}) = \frac{\mu_{\mathcal{M}_{tnk} \rightarrow x_{tnk}}^{(i)}(x_{tnk}) \mu_{x_{tnk} \rightarrow \mathcal{M}_{tnk}}^{(i)}(x_{tnk})}{\sum_{x_{tnk} \in \mathcal{A}} \mu_{\mathcal{M}_{tnk} \rightarrow x_{tnk}}^{(i)}(x_{tnk}) \mu_{x_{tnk} \rightarrow \mathcal{M}_{tnk}}^{(i)}(x_{tnk})}. \quad (59)$$

The local belief $\beta_{x_{tnk}}^{(i)}(x_{tnk})$ can be projected onto a Gaussian PDF denoted by $\hat{\beta}_{x_{tnk}}^{(i)}(x_{tnk}) = \mathcal{N}_{\mathbb{C}}(x_{tnk}; \hat{x}_{x_{tnk}}^{(i)}, \nu_{x_{tnk}}^{(i)})$, where

$$\hat{x}_{x_{tnk}}^{(i)} = \sum_{\alpha_s \in \mathcal{A}} \alpha_s \beta_{x_{tnk}}^{(i)}(x_{tnk} = \alpha_s), \quad (60)$$

$$\nu_{x_{tnk}}^{(i)} = \sum_{\alpha_s \in \mathcal{A}} |\alpha_s|^2 \beta_{x_{tnk}}^{(i)}(x_{tnk} = \alpha_s) - |\hat{x}_{x_{tnk}}^{(i)}|^2, \quad (61)$$

and then the message $\mu_{x_{tnk} \rightarrow f_{tnk}}^{(i)}(x_{tnk})$ is approximated by [38]

$$\hat{\mu}_{x_{tnk} \rightarrow f_{tnk}}^{(i)}(x_{tnk}) \approx \frac{\hat{\beta}_{x_{tnk}}^{(i)}(x_{tnk})}{\mu_{f_{tnk} \rightarrow x_{tnk}}^{(i)}(x_{tnk})} \propto \mathcal{N}_{\mathbb{C}}\left(x_{tnk}; \hat{x}_{x_{tnk} \rightarrow f_{tnk}}^{(i)}, \nu_{x_{tnk} \rightarrow f_{tnk}}^{(i)}\right), \quad (62)$$

where

$$\nu_{x_{tnk} \rightarrow f_{tnk}}^{(i)} = \nu_{x_{tnk}}^{(i)} \frac{\nu_{f_{tnk} \rightarrow x_{tnk}}^{(i)}}{\nu_{f_{tnk} \rightarrow x_{tnk}}^{(i)} - \nu_{x_{tnk}}^{(i)}}, \quad (63)$$

$$\begin{aligned}
& \forall t, m, k, n: z_{f_{tmk} \rightarrow x_{tnk}}^{(i)} = y_{tmk} - \sum_{n' \neq n} \hat{w}_{w_{mn'k} \rightarrow f_{tmk}}^{(i-1)} \hat{x}_{x_{tn'k} \rightarrow f_{tmk}}^{(i-1)}; \\
& \forall t, m, k, n: \tau_{f_{tmk} \rightarrow x_{tnk}}^{(i)} = \sigma_{\varpi}^2 + \sum_{n' \neq n} \left(\left| \hat{w}_{w_{mn'k} \rightarrow f_{tmk}}^{(i-1)} \right|^2 \nu_{x_{tn'k} \rightarrow f_{tmk}}^{(i-1)} + \nu_{w_{mn'k} \rightarrow f_{tmk}}^{(i-1)} \left| \hat{x}_{x_{tn'k} \rightarrow f_{tmk}}^{(i-1)} \right|^2 + \nu_{w_{mn'k} \rightarrow f_{tmk}}^{(i-1)} \nu_{x_{tn'k} \rightarrow f_{tmk}}^{(i-1)} \right) \\
& \forall t, m, k, n: \hat{z}_{f_{tmk} \rightarrow w_{mnk}}^{(i)} = z_{f_{tmk} \rightarrow x_{tnk}}^{(i)} - \hat{x}_{x_{tnk} \rightarrow f_{tmk}}^{(i-1)} \hat{w}_{w_{mnk}}^{(i-1)}; \hat{z}_{f_{tmk} \rightarrow x_{tnk}}^{(i)} = z_{f_{tmk} \rightarrow x_{tnk}}^{(i)} - \hat{w}_{w_{mnk} \rightarrow f_{tmk}}^{(i-1)} \hat{x}_{x_{tnk}}^{(i-1)}; \\
& \forall t, m, k, n: \hat{\tau}_{f_{tmk} \rightarrow w_{mnk}}^{(i)} = \tau_{f_{tmk} \rightarrow x_{tnk}}^{(i)} + \nu_{x_{tnk} \rightarrow f_{tmk}}^{(i-1)} \left| \hat{w}_{w_{mnk}}^{(i-1)} \right|^2; \hat{\tau}_{f_{tmk} \rightarrow x_{tnk}}^{(i)} = \tau_{f_{tmk} \rightarrow x_{tnk}}^{(i)} + \nu_{w_{mnk} \rightarrow f_{tmk}}^{(i-1)} \left| \hat{x}_{x_{tnk}}^{(i-1)} \right|^2; \\
& \forall t, m, k, n: \nu_{f_{tmk} \rightarrow x_{tnk}}^{(i)} = \frac{\hat{\tau}_{f_{tmk} \rightarrow x_{tnk}}^{(i)}}{\left| \hat{w}_{w_{mnk} \rightarrow f_{tmk}}^{(i-1)} \right|^2 + \nu_{w_{mnk} \rightarrow f_{tmk}}^{(i-1)} \left(1 - \frac{\left| \hat{z}_{f_{tmk} \rightarrow x_{tnk}}^{(i)} \right|^2}{\hat{\tau}_{f_{tmk} \rightarrow x_{tnk}}^{(i)}} \right)}; \hat{z}_{f_{tmk} \rightarrow x_{tnk}}^{(i)} = \nu_{f_{tmk} \rightarrow x_{tnk}}^{(i)} \frac{\left(\hat{w}_{w_{mnk} \rightarrow f_{tmk}}^{(i-1)} \right)^* z_{f_{tmk} \rightarrow x_{tnk}}^{(i)}}{\hat{\tau}_{f_{tmk} \rightarrow x_{tnk}}^{(i)}}; \\
& \forall t, m, k, n: \nu_{f_{tmk} \rightarrow w_{mnk}}^{(i)} = \frac{\hat{\tau}_{f_{tmk} \rightarrow w_{mnk}}^{(i)}}{\left| \hat{x}_{x_{tnk} \rightarrow f_{tmk}}^{(i-1)} \right|^2 + \nu_{x_{tnk} \rightarrow f_{tmk}}^{(i-1)} \left(1 - \frac{\left| \hat{z}_{f_{tmk} \rightarrow w_{mnk}}^{(i)} \right|^2}{\hat{\tau}_{f_{tmk} \rightarrow w_{mnk}}^{(i)}} \right)}; \hat{w}_{f_{tmk} \rightarrow w_{mnk}}^{(i)} = \nu_{f_{tmk} \rightarrow w_{mnk}}^{(i)} \frac{\left(\hat{x}_{x_{tnk} \rightarrow f_{tmk}}^{(i-1)} \right)^* z_{f_{tmk} \rightarrow x_{tnk}}^{(i)}}{\hat{\tau}_{f_{tmk} \rightarrow w_{mnk}}^{(i)}}; \\
& \forall t, n, k: \gamma_{x_{tnk}}^{(i)} = \frac{1}{\sum_m \frac{1}{\nu_{f_{tmk} \rightarrow x_{tnk}}^{(i)}}}; \zeta_{x_{tnk}}^{(i)} = \gamma_{x_{tnk}}^{(i)} \sum_m \frac{\hat{x}_{f_{tmk} \rightarrow x_{tnk}}^{(i)}}{\nu_{f_{tmk} \rightarrow x_{tnk}}^{(i)}}; \mu_{x_{tnk} \rightarrow \mathcal{M}_{tnk}}^{(i)}(x_{tnk}) = \mathcal{N}_{\mathbb{C}}(x_{tnk}; \zeta_{x_{tnk}}^{(i)}, \gamma_{x_{tnk}}^{(i)}); \\
& \forall t, n, k, q: \lambda_e^{(i)}(c_{tnk}^q) = \ln \frac{\sum_{x_{tn}^k \in \mathcal{A}_q^1} \mu_{x_{tnk} \rightarrow \mathcal{M}_{tnk}}^{(i)}(x_{tnk}) \mu_{\mathcal{M}_{tnk} \rightarrow x_{tnk}}^{(i-1)}(x_{tnk})}{\sum_{x_{tn}^k \in \mathcal{A}_q^0} \mu_{x_{tnk} \rightarrow \mathcal{M}_{tnk}}^{(i)}(x_{tnk}) \mu_{\mathcal{M}_{tnk} \rightarrow x_{tnk}}^{(i-1)}(x_{tnk})} - \lambda_a^{(i-1)}(c_{tnk}^q) \\
& \forall n: \text{Decode and generate LLRs } \left\{ \lambda_a^{(i)}(c_{tnk}^q), \forall t, \forall k, \forall q \right\} \\
& \forall t, n, k: \mu_{\mathcal{M}_{tnk} \rightarrow x_{tnk}}^{(i)}(x_{tnk}) = \prod_q \frac{\exp\left(c_{tnk}^q \lambda_a^{(i)}(c_{tnk}^q)\right)}{1 + \exp\left(c_{tnk}^q \lambda_a^{(i)}(c_{tnk}^q)\right)}; \beta_{x_{tnk}}^{(i)}(x_{tnk}) = \frac{\mu_{\mathcal{M}_{tnk} \rightarrow x_{tnk}}^{(i)}(x_{tnk}) \mu_{x_{tnk} \rightarrow \mathcal{M}_{tnk}}^{(i)}(x_{tnk})}{\sum_{x_{tnk} \in \mathcal{A}} \mu_{\mathcal{M}_{tnk} \rightarrow x_{tnk}}^{(i)}(x_{tnk}) \mu_{x_{tnk} \rightarrow \mathcal{M}_{tnk}}^{(i)}(x_{tnk})}; \\
& \forall t, n, k: \hat{x}_{x_{tnk}}^{(i)} = \sum_{\alpha_s \in \mathcal{A}} \alpha_s \beta_{x_{tnk}}^{(i)}(x_{tnk} = \alpha_s); \nu_{x_{tnk}}^{(i)} = \sum_{\alpha_s \in \mathcal{A}} |\alpha_s|^2 \beta_{x_{tnk}}^{(i)}(x_{tnk} = \alpha_s) - \left| \hat{x}_{x_{tnk}}^{(i)} \right|^2; \\
& \forall t, n, k, m: \nu_{x_{tnk} \rightarrow f_{tmk}}^{(i)} = \nu_{x_{tnk}}^{(i)} \frac{\nu_{f_{tmk} \rightarrow x_{tnk}}^{(i)}}{\nu_{f_{tmk} \rightarrow x_{tnk}}^{(i)} - \nu_{x_{tnk}}^{(i)}}, \forall m: \hat{x}_{x_{tnk} \rightarrow f_{tmk}}^{(i)} = \hat{x}_{x_{tnk}}^{(i)} + \nu_{x_{tnk}}^{(i)} \frac{\hat{x}_{x_{tnk}}^{(i)} - \hat{x}_{f_{tmk} \rightarrow x_{tnk}}^{(i)}}{\nu_{f_{tmk} \rightarrow x_{tnk}}^{(i)} - \nu_{x_{tnk}}^{(i)}}.
\end{aligned}$$

Table I: The EP-QA at the i th turbo iteration.

$$\hat{x}_{x_{tnk} \rightarrow f_{tmk}}^{(i)} = \hat{x}_{x_{tnk}}^{(i)} + \nu_{x_{tnk}}^{(i)} \frac{\hat{x}_{x_{tnk}}^{(i)} - \hat{x}_{f_{tmk} \rightarrow x_{tnk}}^{(i)}}{\nu_{f_{tmk} \rightarrow x_{tnk}}^{(i)} - \nu_{x_{tnk}}^{(i)}}. \quad (64)$$

Summing up the above discussions, the EP based message passing for the *detection-decoding-loop* is formulated in Table I, which will be referred to as “EP-QA”. At the first turbo iteration, we set $\hat{x}_{x_{tnk} \rightarrow f_{tmk}}^{(0)} = 0$, $\nu_{x_{tnk} \rightarrow f_{tmk}}^{(0)} = 1$, $\forall t, n, k, m$; $\hat{w}_{w_{mnk} \rightarrow f_{tmk}}^{(0)} = 0$, $\nu_{w_{mnk} \rightarrow f_{tmk}}^{(0)} = 1$, $\forall t, m, k, n$; and $\lambda_a^{(0)}(c_{tnk}^q) = 0$, $\forall t, n, k, q$. When updating messages, it can be observed that the variance parameters $\nu_{f_{tmk} \rightarrow w_{mnk}}^{(i)}$ in (45) and $\nu_{x_{tnk} \rightarrow f_{tmk}}^{(i)}$ in (63) take negative values in rare situations, which can lead to erratic behavior and is common in many EP implementations [30]. To circumvent this problem, we change a negative $\nu_{f_{tmk} \rightarrow w_{mnk}}^{(i)}$ to $+\infty$ (a large positive constant is used in

$$\begin{aligned}
\forall m,n,k: z_{g_{mnk}}^{(i)} &= \hat{w}_{w_{mnk} \rightarrow g_{mnk}}^{(i)} - \sum_l \phi_{kl} \hat{h}_{h_{mnk}}^{(i-1)} + \epsilon_{mnk}^{(i-1)}; \tau_{g_{mnk}}^{(i)} = \nu_{w_{mnk} \rightarrow g_{mnk}}^{(i)} + \sum_l \nu_{h_{mnk}}^{(i-1)}. \\
\forall mn: \tau_{mn}^{(i)} &= \sum_k \tau_{g_{mnk}}^{(i)} / K. \\
\forall m,n,l: \xi_{mnk}^{(i)} &= \sum_k \frac{\Phi_{kl}^* z_{g_{mnk}}^{(i)}}{\tau_{g_{mnk}}^{(i)}} + \hat{h}_{h_{mnk}}^{(i-1)} \sum_{k'} \frac{1}{\tau_{g_{mnk}}^{(i)}} - \frac{\nu_{h_{mnk}}^{(i-1)}}{\tau_{mn}^{(i)}} \xi_{mnk}^{(i-1)}; \nu_{h_{mnk}}^{(i)} = \frac{1}{\sum_{m'} \left(\left| \hat{h}_{h_{m'n}^{(i-1)}} \right|^2 + \nu_{h_{m'n}^{(i-1)}}^{(i-1)} \right)}; \hat{h}_{h_{mnk}}^{(i)} = \nu_{h_{mnk}}^{(i)} \xi_{mnk}^{(i)}. \\
\forall mn: \nu_{mn}^{(i)} &= \sum_l \nu_{h_{mnk}}^{(i)} / L. \\
\forall m,n,k: \epsilon_{mnk}^{(i)} &= \frac{z_{g_{mnk}}^{(i)} \sum_l \nu_{h_{mnk}}^{(i)} + \sum_{l'} \phi_{kl'} \nu_{h_{mnk}}^{(i)} \hat{h}_{h_{mnk}}^{(i-1)} - \bar{\nu}_{mn}^{(i)} \epsilon_{mnk}^{(i-1)}}{\tau_{g_{mnk}}^{(i)}}; \hat{w}_{g_{mnk} \rightarrow w_{mnk}}^{(i)} = \sum_l \phi_{kl} \hat{h}_{h_{mnk}}^{(i)} - \epsilon_{mnk}^{(i)}; \nu_{g_{mnk} \rightarrow w_{mnk}}^{(i)} = \sum_l \nu_{h_{mnk}}^{(i)}. \\
\forall m,n,k: \nu_{w_{mnk}}^{(i)} &= \frac{1}{\nu_{g_{mnk} \rightarrow w_{mnk}}^{(i)} + \sum_t \frac{1}{\nu_{f_{tmk} \rightarrow w_{mnk}}^{(i)}}}, \hat{w}_{w_{mnk}}^{(i)} = \nu_{w_{mnk}}^{(i)} \left(\frac{\hat{w}_{g_{mnk} \rightarrow w_{mnk}}^{(i)}}{\nu_{g_{mnk} \rightarrow w_{mnk}}^{(i)}} + \sum_t \frac{\hat{w}_{f_{tmk} \rightarrow w_{mnk}}^{(i)}}{\nu_{f_{tmk} \rightarrow w_{mnk}}^{(i)}} \right). \\
\forall m,n,k,t: \nu_{w_{mnk} \rightarrow f_{tmk}}^{(i)} &= \frac{1}{\nu_{w_{mnk}}^{(i)} - \frac{1}{\nu_{f_{tmk} \rightarrow w_{mnk}}^{(i)}}}, \hat{w}_{w_{mnk} \rightarrow f_{tmk}}^{(i)} = \nu_{w_{mnk} \rightarrow f_{tmk}}^{(i)} \left(\frac{\nu_{w_{mnk}}^{(i)}}{\hat{w}_{w_{mnk}}^{(i)}} - \frac{\hat{w}_{f_{tmk} \rightarrow w_{mnk}}^{(i)}}{\nu_{f_{tmk} \rightarrow w_{mnk}}^{(i)}} \right).
\end{aligned}

---$$

Table II: The GMP at the i th turbo iteration.

practice, e.g., 10^6 , see [39] and [40]) and change a negative $\nu_{x_{tnk} \rightarrow f_{tmk}}^{(i)}$ to $\nu_{x_{tnk}}^{(i)}$ shown in (61). Although this is just a heuristic measure, in our simulations it indeed avoids the instability of expectation propagation.

B. Message Updating in Channel-Estimation-Loop

Now we focus on Bayesian learning of the hyper-parameters $\{\gamma_{nl}\}$, as it is unknown to the receiver. Using the variational message-passing rule [41], we obtain the message from the function node ψ_{mnk} to the precision variable γ_{nl} ,

$$\mu_{\psi_{mnk} \rightarrow \gamma_{nl}}^{(i)}(\gamma_{nl}) = \exp \left(\mathbb{E}_{\beta_{h_{mnk}}^{(i-1)}(h_{mnk})} \ln \psi_{mnk}(h_{mnk}, \gamma_{nl}) \right) \propto \text{Gam} \left(\gamma_{nl}; 0, |\hat{h}_{h_{mnk}}^{(i-1)}|^2 + \nu_{h_{mnk}}^{(i-1)} \right), \quad (65)$$

where $\beta_{h_{mnk}}^{(i-1)}(h_{mnk}) = \mathcal{N}_{\mathbb{C}}(h_{mnk}; \hat{h}_{h_{mnk}}^{(i-1)}, \nu_{h_{mnk}}^{(i-1)})$ is the belief of h_{mnk} at the $(i-1)$ th turbo iteration. Then the belief of precision variable γ_{nl} is updated by

$$\beta_{\gamma_{nl}}^{(i)}(\gamma_{nl}) = p(\gamma_{nl}) \prod_m \mu_{\psi_{mnk} \rightarrow \gamma_{nl}}^{(i)}(\gamma_{nl}) \propto \text{Gam} \left(\gamma_{nl}; M, \sum_m \left(|\hat{h}_{h_{mnk}}^{(i-1)}|^2 + \nu_{h_{mnk}}^{(i-1)} \right) \right), \quad (66)$$

Using the variational message-passing rule again, the message from the function node $\psi_{mnk}(h_{mnk}, \gamma_{nl})$ to variable node h_{mnk} reads

$$\mu_{\psi_{mnk} \rightarrow h_{mnk}}^{(i)}(h_{mnk}) = \exp \left(\mathbb{E}_{\beta_{\gamma_{nl}}^{(i)}(\gamma_{nl})} \ln \psi_{mnk}(h_{mnk}, \gamma_{nl}) \right) \propto \mathcal{N}_{\mathbb{C}} \left(h_{mnk}; 0, \frac{1}{M} \sum_m \left(|\hat{h}_{h_{mnk}}^{(i-1)}|^2 + \nu_{h_{mnk}}^{(i-1)} \right) \right), \quad (67)$$

and the belief of h_{mnl} is updated by $\beta_{h_{mnl}}^{(i)}(h_{mnl}) = \mu_{\psi_{mnl} \rightarrow h_{mnl}}^{(i)}(h_{mnl}) \prod_k \mu_{g_{mnk} \rightarrow h_{mnl}}^{(i)}(h_{mnl})$, where $\mu_{g_{mnk} \rightarrow h_{mnl}}^{(i)}(h_{mnl})$ is the message from g_{mnk} to h_{mnl} .

Following the derivation in [31], the Gaussian message passing for channel-estimation task, i.e., updating $\{\nu_{w_{mnk} \rightarrow f_{tmk}}^{(i)}, \hat{w}_{w_{mnk} \rightarrow f_{tmk}}^{(i)}\}$, is given by Table II, which will be referred to as “GMP”. At the first turbo iteration, i.e., $i = 1$, we set $|\hat{h}_{h_{mnl}}^{(0)}|^2 + \nu_{h_{mnl}}^{(0)} = 1/L, \forall m, n, l$, and $\xi_{mnl}^{(0)} = 0, \forall m, n, l$.

IV. COMPLEXITY COMPARISONS

Table III: Complexity of detection and decoding per turbo iteration in terms of FLOPs.

Algorithm	FLOPs per Iteration
EP-QA-L / EP-QA	$47TMNK + (11N + 4)M(K - K_p) + (23 \mathcal{A} + 3Q \mathcal{A} + Q)TNK$
BP-GA [8], [16]	$(28 \mathcal{A} + 33)TMNK + (2 \mathcal{A} + 3Q \mathcal{A} + Q)TNK$
BP-MF [18]	$19TMNK + (11N + 4)M(K - K_p) + (23 \mathcal{A} + 3Q \mathcal{A} + Q)TNK$
BP-MF-M [29]	$33TMNK + (11N + 4)M(K - K_p) + (23 \mathcal{A} + 3Q \mathcal{A} + Q)TNK$

Table IV: Complexity of channel estimation per turbo iteration in terms of FLOPs.

Algorithm	FLOPs per Iteration
EP-QA-L	$MN(20K\log_2 K + 30TK + 11K - 26TK_p + 13K_p + 18L - 2)$
EP-QA / BP-GA	$MN(20K\log_2 K + 30TK + 11K - 26TK_p + 13K_p + 14L - 2)$
BP-MF [18]	$MN(16K^3 + 12K^2 + 17TK - K) + 2TNK - 2NK - 2MN$
BP-MF-M [29]	$MN(118G^2 + 68G - 4)K - 112G^3 - 92G^3 + 5G$

In the following, EP-QA-L denotes the joint algorithm using the EP-QA shown in Table I to complete detection and decoding and using the GMP shown in Table II to complete channel estimation; EP-QA and BP-GA denote the joint algorithms using the EP-QA shown in Table I and the BP-GA ((22)-(34)) to complete detection and decoding, respectively, and both using the GMP with oracle PDP to complete channel estimation, i.e., the term $\frac{1}{M} \sum_m (|\hat{h}_{h_{mnl}}^{(i-1)}|^2 + \nu_{h_{mnl}}^{(i-1)})$ in (67) is replaced by the true path power of h_{mnl} ; the BP-MF denotes the BP-MF algorithm employing disjoint channel model proposed in [18] and [22]; and BP-MF-M denotes the low-complexity version of BP-MF algorithm employing Markov channel model proposed in [29]. Note that, both the BP-MF and the BP-MF-M require prior knowledge of the channel PDP. We compare the

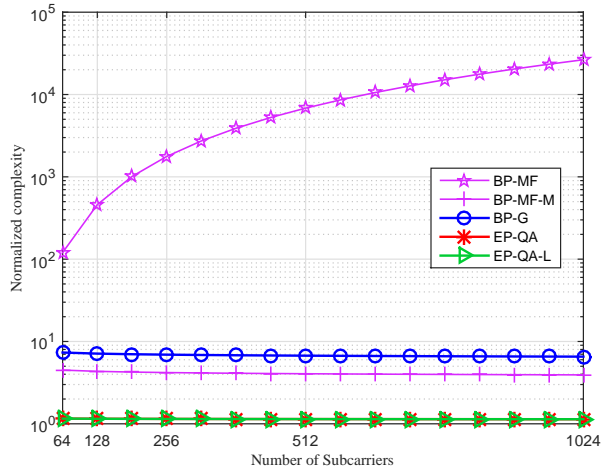


Figure 2: Normalized complexity of joint algorithms versus the number of subcarriers K in a 64×8 MIMO-OFDM systems with 16QAM, where $K_p = L = K/8$, and $T = 8$. The complexity is normalized over the complexity of joint algorithm EP-QA-L.

complexity of our proposed EP-QA-L algorithm with that of the EP-QA, the BP-GA, the BP-MF, and the BP-MF-M. The complexity is evaluated in terms of floating-point operations (FLOPs) per iteration. Here we do not distinguish the complexity of addition, subtraction, multiplication, and division for simplicity. Note that the multiplication of a complex number and a real number needs two FLOPs, and the multiplication of two complex numbers (excluding conjugate numbers) needs six FLOPs. It is assumed that the operation of $\exp(\cdot)$ can be implemented by a look-up table and $\{\lambda_e^{(i)}(c_{tnk}^q)\}$ is calculated by the decoders, which are not taken into account. Table III shows the complexity of these algorithms performing detection and decoding. For channel estimation, the complexity is listed in Table IV. The normalized complexity of these joint algorithms per turbo iteration versus number of subcarriers K in a 64×8 MIMO-OFDM systems with 16QAM is shown in Fig 2, where $K_p = L = K/8$ and $T = 8$. The EP-QA-L and EP-QA have almost the same complexity, while the EP-Q has the lowest complexity. As the number of subcarriers increases from 64 to 1024, the complexity of EP-QA-L is about $\frac{1}{3}$ of that of BP-MF-M, about $\frac{1}{6}$ of that of BP-G, and about $\frac{1}{100} \sim \frac{1}{23000}$ of that of BP-MF.

V. SIMULATION RESULTS

The proposed EP-QA-L is compared with the EP-QA, the BP-MF, the BP-MF-M, and the BP-GA in terms of normalized mean square error (NMSE) of the channel weights and BER, as well as the matched filter bound (MFB) that is obtained by the MAP decoding under the condition of perfect multiuser interference cancellation and perfect channel state information (PCSI).

Due to space constraints, a selected set of system parameters is used for simulations¹. We consider the uplink of a multiuser system with $N = 8$ independent users, and each user is equipped with one transmit antenna. For each user, the transmission is based on OFDM with $K = 128$ subcarriers. We choose a $R = 1/2$ recursive systematic convolutional (RSC) code with generator polynomial $[G_1, G_2] = [117, 155]_{\text{oct}}$, followed by a random interleaver. For bit-to-symbol mapping, multilevel Gray-mapping is used [20]. The maximum multipath delay $L = 16$ is assumed and the PDP is modeled as exponentially decaying, i.e., $\gamma_{nl} = \frac{e^{-l/6}}{\sum_{l=1}^L e^{-l/6}}, \forall n$. The CP length is set to be $L_{\text{cp}} = L$ and the pilot length is also set to be $K_p = 16$. We adopt the channel model in (1) with the spatial correlation matrix in (2). Considering a massive (16×4) UPA and a moderate (16×1) unformed linear array (ULA), we set the antenna spacing to $d_{\text{az}} = d_{\text{el}} = \lambda$, uniformly generate following random variables independently for each user in a channel realization: the mean of horizontal AoD θ_{az} in $[\pi/6, 5\pi/6]$, the mean of vertical AoD θ_{el} in $[\pi/12, \pi/3]$, and the standard deviations of horizontal AoD $\sqrt{\nu_{\text{az}}}$ and vertical AoD $\sqrt{\nu_{\text{el}}}$ both in $[\pi/12, \pi/6]$. At the receiver, the BCJR algorithm is used to decode the convolutional codes. The channels are assumed to be block-static for the selected $T = 8$ transmitted OFDM symbols.

Taking into account of the overhead incurred by the CP and the frequency-domain pilots, the spectral efficiency η of the MIMO-OFDM scheme normalized by the ideal case without any overhead is expressed as $\eta = \frac{TNK - N^2K_p}{TN(L_{\text{cp}} + K)} = 77.8\%$ [35]. The energy per bit to noise power spectral density ratio E_b/N_0 is defined as [42]

$$\frac{E_b}{N_0} = \frac{E_s}{N_0} + 10 \log_{10} \frac{M}{\eta RNQ}, \quad (68)$$

¹We will make our simulation package available for download after (possible) acceptance of the paper.

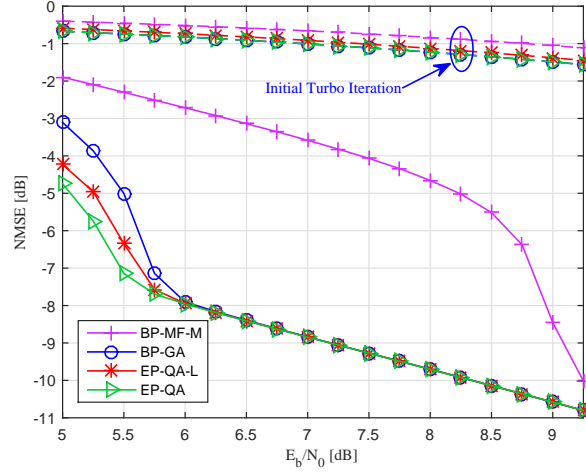


Figure 3: NMSE versus E_b/N_0 in the 64×8 MIMO system with 16QAM.

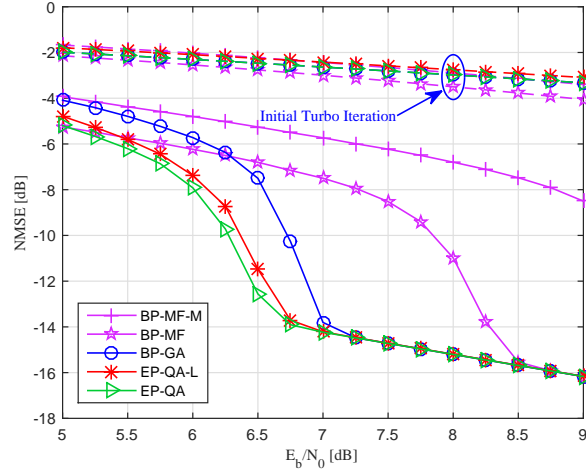


Figure 4: NMSE versus E_b/N_0 in the 16×8 MIMO system with 16QAM.

where E_s/N is the average energy per transmitted symbol. For a fixed E_b/N_0 , then E_s/N_0 is scaled down by the number of receive antennas M .

A. Channel-Tap NMSE Versus E_b/N_0

In the initial turbo iteration, only the pilot symbols are available for the channel estimation. For the EP-QA-L and the EP-QA, the channel estimation loops perform 5 inner iterations in the initial turbo iteration and perform only 1 inner iteration in each of the following turbo iterations.

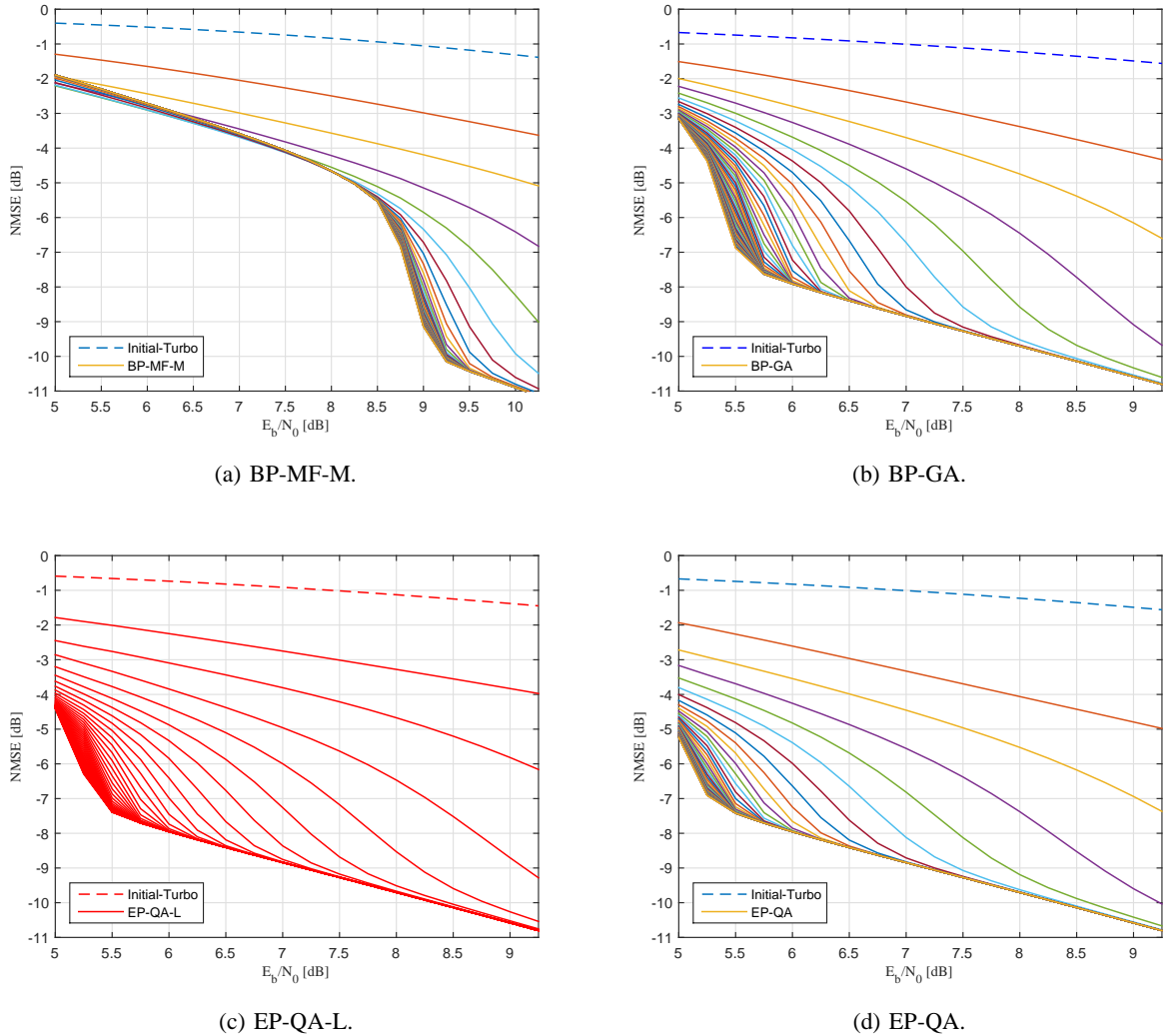


Figure 5: NMSE versus E_b/N_0 with multiple iterations in the 64×8 MIMO system with 16QAM.

For the BP-MF, the channel estimator is equivalent to a pilot-based LMMSE estimator in the initial turbo iteration, and becomes a data-aided LMMSE in the next turbo iterations. The channel estimation of the BP-MF-M is performed by a Kalman smoother proposed in [29], where the group-size of contiguous channel weights is set to be $G = 4$.

Fig. 3 and Fig. 4 show the NMSE of the channel estimation versus E_b/N_0 in the 64×8 MIMO system (16×4 UPA) and the 16×8 MIMO system (16×1 ULA), respectively. The

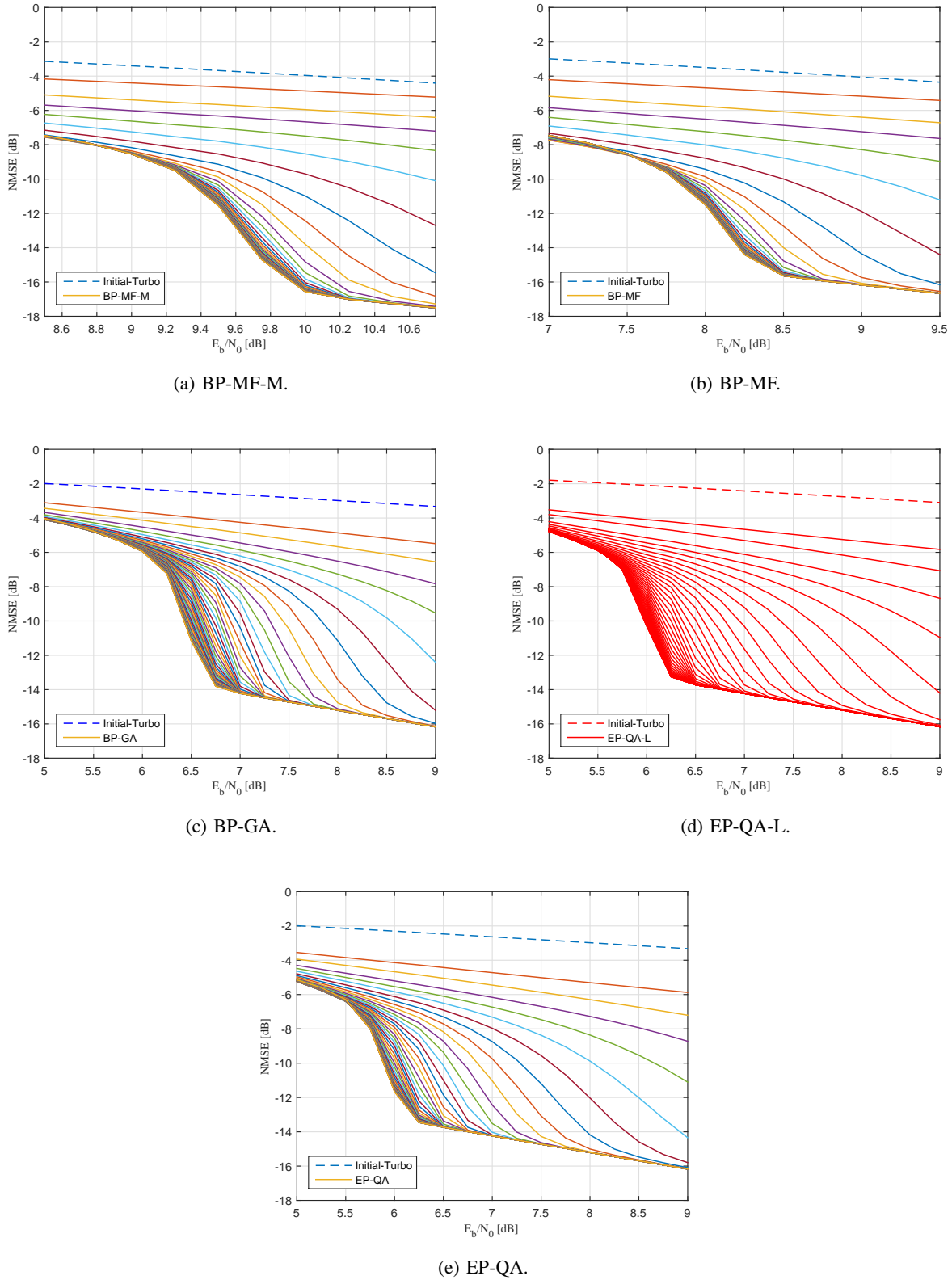


Figure 6: NMSE versus E_b/N_0 with multiple iterations in the 16×8 MIMO system with 16QAM.

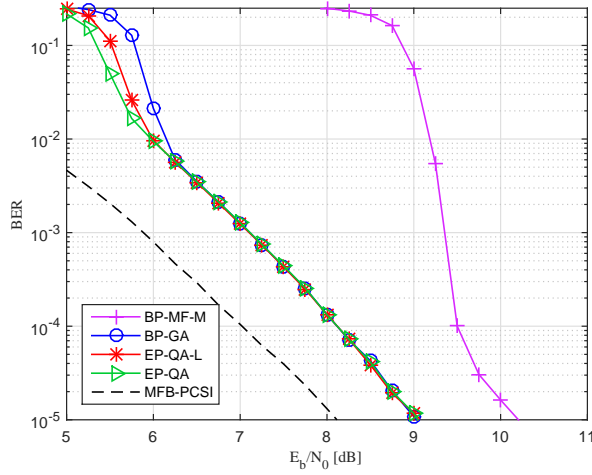


Figure 7: BER versus E_b/N_0 in the 64×8 MIMO system with 16QAM.

NMSE at the i th turbo iteration is calculated by

$$\text{NMSE} = \frac{1}{\Theta} \sum_{\theta=1}^{\Theta} \frac{1}{MN} \sum_{m=1}^M \sum_{n=1}^N \frac{\sum_{l=1}^L |h_{mnl} - \hat{h}_{mnl}^{(i)}|^2}{\sum_{l=1}^L |h_{mnl}|^2}, \quad (69)$$

where Θ is the number of Monte Carlo runs. It is shown that the NMSE of the proposed EP-QA-L outperforms other algorithms including the BP-GA, the BP-MF-M, and the BP-MF (which is evaluated only in the 16×8 MIMO system due to complexity issue). It is also shown that, compared with the EP-QA using oracle channel PDP, the EP-QA-L is slightly degraded only in the low region of E_b/N_0 . The NMSE of BP-MF-M is higher than that of all other algorithms at the point that the number of turbo iterations is 15.

Fig. 5 and Fig. 6 present the NMSE performance with increasing number of turbo iterations. In the high region of E_b/N_0 , it can be seen that 10 turbo iterations are enough for all the algorithms to achieve convergence. In the low E_b/N_0 region, the EP-QA-L (and the EP-QA with oracle PDP) can uniformly improve the NMSE performance by increasing the number of turbo iterations, but other algorithms can't.

B. BER Versus E_b/N_0

Fig. 7 and Fig. 8 show the BER performance versus E_b/N_0 in the 64×8 MIMO system and the 16×8 MIMO system, respectively. The BP-GA, the EP-QA, and the EP-QA-L achieve the

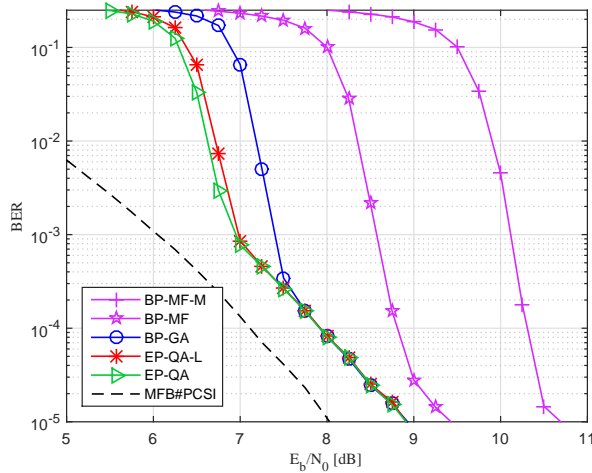


Figure 8: BER versus E_b/N_0 in the 16×8 MIMO system with 16QAM.

same performance that is about 0.9 dB away from the MFB-PCSI at $\text{BER} = 10^{-5}$, but the BP-MF-M is about 2.0 dB away from the MFB-PCSI in the 64×8 MIMO system and 2.6 dB away from the MFB-PCSI in the 16×8 MIMO system. In the 16×8 MIMO system, even the BP-MF with much higher complexity is still inferior to the EP-QA-L about 0.5 dB at $\text{BER} = 10^{-5}$.

Fig. 9 and Fig. 10 show the BER performance versus E_b/N_0 with increasing number of turbo iterations. In the 64×8 MIMO system, to converge at $\text{BER} = 10^{-5}$, the BP-GA, the EP-QA, and the EP-QA-L need about 7 turbo iterations and the BP-MF-M needs about 12 turbo iterations. In the 16×8 MIMO system, the BP-GA, the EP-QA, and the EP-QA-L need 9 turbo iterations to converge at $\text{BER} = 10^{-5}$ and the BP-MF needs about 12 turbo iterations, while the performance of BP-MF-M is somewhat unstable.

VI. CONCLUSION

In this paper, we presented a message-passing receiver for joint channel-estimation and decoding in the 3D massive MIMO systems transmitting over frequency-selective block fading channels. Expectation propagation with quadratic approximation was derived to deal with the decoupling of channel coefficients and data symbols, and a low-complexity Gaussian message-passing algorithm was applied for the channel estimation. It was verified through simulations that in the 3D massive MIMO systems our proposed algorithm could approach to the MFB with limited loss and its complexity is very low.

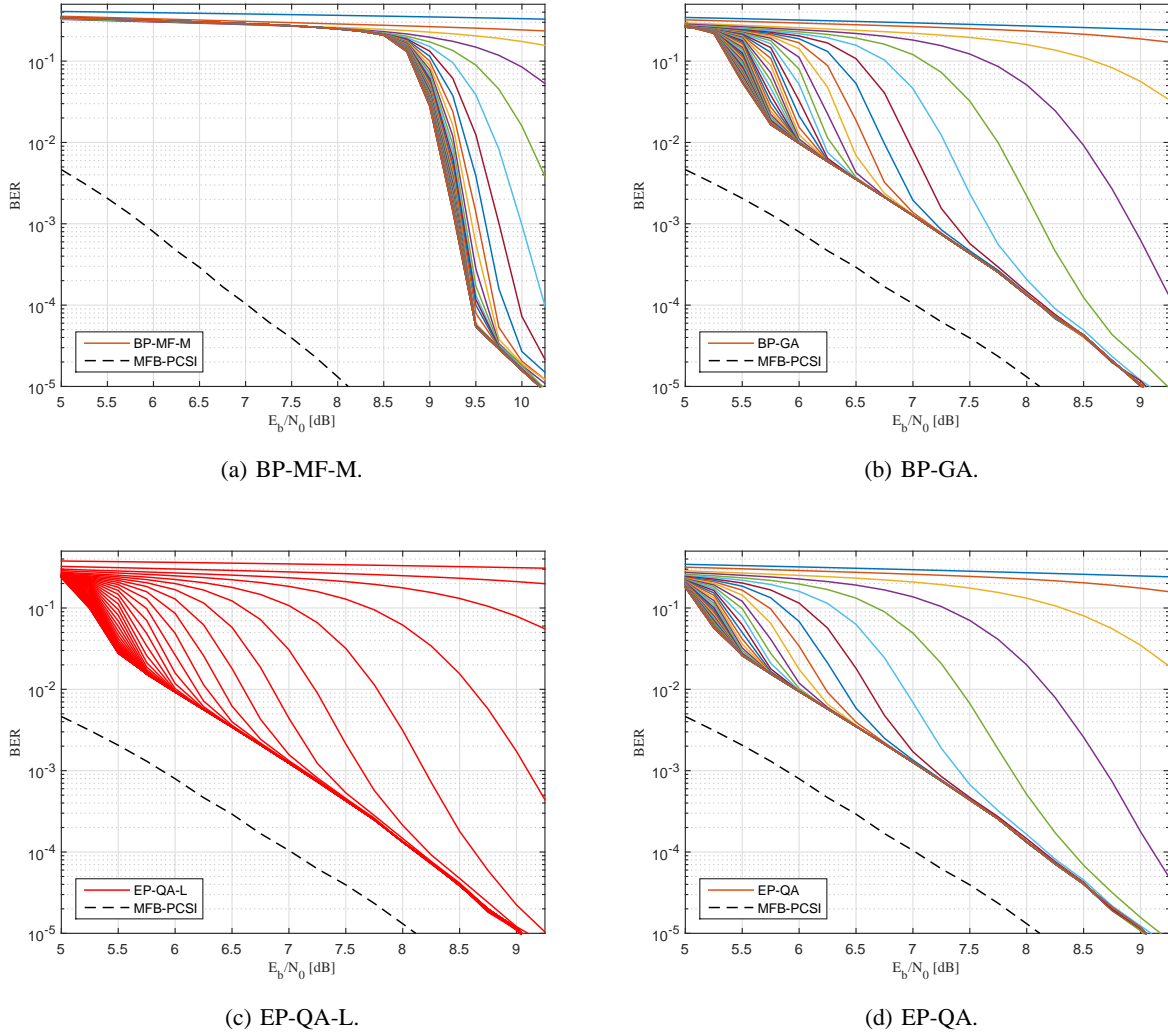


Figure 9: BER versus E_b/N_0 in the 64×8 MIMO system with 16QAM.

ACKNOWLEDGMENT

The authors would like to gratefully acknowledge Prof. P. Schniter for valuable suggestions, especially on the issue of negative variances occurred in the EP algorithm.

APPENDIX

Using the so-called *Wirtinger calculus* [43], [44], a real function of $z \in \mathbb{C}$, $\tau > 0$ and $u \in \mathbb{C}$ is defined by

$$\mathcal{H}(\vec{z}, \tau, \vec{u}) = \frac{|z|^2}{\tau} + \ln \tau + \frac{|u|^2}{\nu}, \quad (70)$$

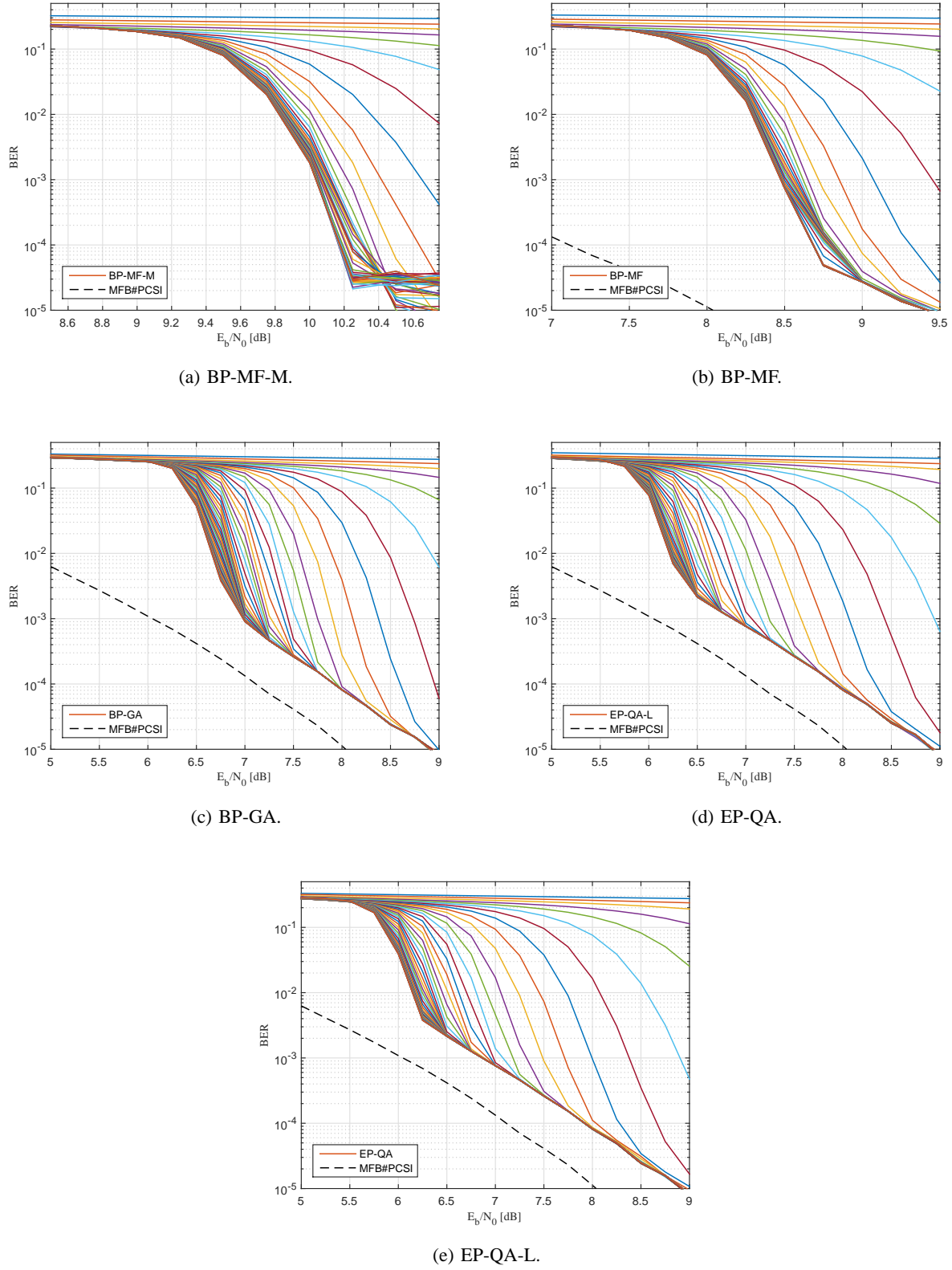


Figure 10: BER versus E_b/N_0 in the 16×8 MIMO system with 16QAM.

where the conjugate coordinates \vec{z} and \vec{u} are defined by $\vec{z} \triangleq [z, z^*]^\top$ and $\vec{u} \triangleq [u, u^*]^\top$ respectively, and $\nu > 0$ is a constant. For the function $\mathcal{H}(\vec{z}, \tau, \vec{u})$, some of its partial derivations are given by

$$\frac{\partial \mathcal{H}}{\partial \vec{z}} \triangleq \left[\frac{\partial \mathcal{H}}{\partial z}, \frac{\partial \mathcal{H}}{\partial z^*} \right] = \left[\frac{z^*}{\tau}, \frac{z}{\tau} \right], \quad (71)$$

$$\frac{\partial^2 \mathcal{H}}{\partial \vec{z} \partial \vec{z}} \triangleq \left[\begin{array}{cc} \frac{\partial}{\partial z} \left(\frac{\partial \mathcal{H}}{\partial z} \right)^* & \frac{\partial}{\partial z^*} \left(\frac{\partial \mathcal{H}}{\partial z} \right)^* \\ \frac{\partial}{\partial z} \left(\frac{\partial \mathcal{H}}{\partial z^*} \right)^* & \frac{\partial}{\partial z^*} \left(\frac{\partial \mathcal{H}}{\partial z^*} \right)^* \end{array} \right] = \left[\begin{array}{cc} \frac{1}{\tau} & 0 \\ 0 & \frac{1}{\tau} \end{array} \right], \quad (72)$$

$$\frac{\partial \mathcal{H}}{\partial \tau} = \frac{1}{\tau} - \frac{|z|^2}{\tau^2}, \quad (73)$$

$$\frac{\partial \mathcal{H}}{\partial \vec{u}} \triangleq \left[\frac{\partial \mathcal{H}}{\partial u}, \frac{\partial \mathcal{H}}{\partial u^*} \right] = \left[\frac{u^*}{\nu}, \frac{u}{\nu} \right], \quad (74)$$

$$\frac{\partial^2 \mathcal{H}}{\partial \vec{u} \partial \vec{u}} \triangleq \left[\begin{array}{cc} \frac{\partial}{\partial u} \left(\frac{\partial \mathcal{H}}{\partial u} \right)^* & \frac{\partial}{\partial u^*} \left(\frac{\partial \mathcal{H}}{\partial u} \right)^* \\ \frac{\partial}{\partial u} \left(\frac{\partial \mathcal{H}}{\partial u^*} \right)^* & \frac{\partial}{\partial u^*} \left(\frac{\partial \mathcal{H}}{\partial u^*} \right)^* \end{array} \right] = \left[\begin{array}{cc} \frac{1}{\nu} & 0 \\ 0 & \frac{1}{\nu} \end{array} \right]. \quad (75)$$

Up to the second order, the power series expansion of $\mathcal{H}(\vec{z}, \tau, \vec{u})$ at the point $(\vec{z}_0, \tau_0, \vec{u}_0)$ is given by [44]

$$\begin{aligned} \mathcal{H}(\vec{z}, \tau, \vec{u}) &\approx \mathcal{H}(\vec{z}_0, \tau_0, \vec{u}_0) + \frac{\partial \mathcal{H}}{\partial \vec{z}_0} \Delta \vec{z} + \frac{\partial \mathcal{H}}{\partial \tau_0} \Delta \tau + \frac{\partial \mathcal{H}}{\partial \vec{u}_0} \Delta \vec{u} \\ &\quad + \frac{1}{2} (\Delta \vec{z})^\top \frac{\partial^2 \mathcal{H}}{\partial \vec{z}_0 \partial \vec{z}_0} \Delta \vec{z} + \frac{1}{2} (\Delta \vec{u})^\top \frac{\partial^2 \mathcal{H}}{\partial \vec{u}_0 \partial \vec{u}_0} \Delta \vec{u} \\ &= \mathcal{H}(\vec{z}_0, \tau_0, \vec{u}_0) + 2\Re \left\{ \frac{z_0^*}{\tau_0} \Delta z + \frac{u_0^*}{\nu} \Delta u \right\} \\ &\quad - \frac{|z_0|^2}{\tau_0^2} \Delta \tau + \frac{1}{\tau_0} \Delta \tau + \frac{1}{\tau_0} |\Delta z|^2 + \frac{1}{\nu} |\Delta u|^2, \end{aligned} \quad (76)$$

where $\Delta \vec{z} \triangleq \vec{z} - \vec{z}_0$, $\Delta \tau \triangleq \tau - \tau_0$ and $\Delta \vec{u} \triangleq \vec{u} - \vec{u}_0$

REFERENCES

- [1] T. L. Marzetta, "Noncooperative cellular wireless with unlimited numbers of base station antennas," *IEEE Trans. Wireless Commun.*, vol. 9, no. 11, pp. 3590–3600, Nov. 2010.
- [2] F. Rusek, D. Persson, B. K. Lau, E. G. Larsson, T. L. Marzetta, O. Edfors, and F. Tufvesson, "Scaling up MIMO: Opportunities and challenges with very large arrays," *IEEE Signal Process. Mag.*, vol. 30, no. 1, pp. 40–60, Jan. 2013.
- [3] J. Hoydis, S. ten Brink, and M. Debbah, "Massive MIMO in the UL/DL of cellular networks: How many antennas do we need?" *IEEE J. Sel. Areas Commun.*, vol. 31, no. 2, pp. 160–171, Feb. 2013.
- [4] E. G. Larsson, O. Edfors, F. Tufvesson, and T. L. Marzetta, "Massive MIMO for next generation wireless systems," *IEEE Communications Magazine*, vol. 52, no. 2, pp. 186–195, February 2014.

- [5] N. Shariati, E. Björnson, M. Bengtsson, and M. Debbah, "Low-complexity polynomial channel estimation in large-scale MIMO with arbitrary statistics," *IEEE J. Sel. Topics in Signal Process.*, vol. 8, no. 5, pp. 815–830, Oct. 2014.
- [6] S. Noh, M. D. Zoltowski, Y. Sung, and D. J. Love, "Pilot beam pattern design for channel estimation in massive MIMO systems," *IEEE J. Sel. Topics in Signal Process.*, vol. 8, no. 5, pp. 787–801, Oct. 2014.
- [7] P. S. Rossi and R. R. Müller, "Joint twofold-iterative channel estimation and multiuser detection for MIMO-OFDM systems," *IEEE Trans. Wireless Commun.*, vol. 7, no. 11, pp. 4719–4729, Nov. 2008.
- [8] C. Novak, G. Matz, and F. Hlawatsch, "IDMA for the multiuser MIMO-OFDM uplink: A factor graph framework for joint data detection and channel estimation," *IEEE Trans. Signal Process.*, vol. 61, no. 16, pp. 4051–4066, Aug. 2013.
- [9] Y. Liu, Z. Tan, H. Hu, L. J. Cimini, and G. Y. Li, "Channel estimation for OFDM," *IEEE Communications Surveys & Tutorials*, vol. 16, no. 4, pp. 1891–1908, Fourth Quarter 2014.
- [10] P. Zhang, S. Chen, and L. Hanzo, "Embedded iterative semi-blind channel estimation for three-stage-concatenated MIMO-aided QAM turbo transceivers," *IEEE Trans. Veh. Technol.*, vol. 63, no. 1, pp. 439–446, Jan. 2014.
- [11] J. Ma and P. Li, "Data-aided channel estimation in large antenna systems," *IEEE Trans. Signal Process.*, vol. 62, no. 12, pp. 3111–3124, June 2014.
- [12] S. Park, B. Shim, and J. W. Choi, "Iterative channel estimation using virtual pilot signals for MIMO-OFDM systems," *IEEE Trans. Signal Process.*, vol. 63, no. 12, pp. 3032–3045, June 2015.
- [13] F. R. Kschischang, B. J. Frey, and H.-A. Loeliger, "Factor graphs and the sum-product algorithm," *IEEE Trans. Inf. Theory*, vol. 47, no. 2, pp. 498–519, Feb. 2001.
- [14] A. P. Worthen and W. E. Stark, "Unified design of iterative receivers using factor graphs," *IEEE Trans. Inf. Theory*, vol. 47, no. 2, pp. 843–849, 2001.
- [15] H. Wymeersch, *Iterative Receiver Design*. Cambridge, U.K.: Cambridge Univ. Press, 2007.
- [16] Y. Liu, L. Brunel, and J. J. Boutros, "Joint channel estimation and decoding using Gaussian approximation in a factor graph over multipath channel," in *Proc. Int. Symp. on Personal, Indoor and Mobile Radio Commun. (PIMRC)*, 2009, pp. 3164–3168.
- [17] G. E. Kirkelund, C. N. Manchón, L. P. B. Christensen, E. Riegler, and B. H. Fleury, "Variational message-passing for joint channel estimation and decoding in MIMO-OFDM," in *Proc. IEEE Global Telecomm. Conf. (GLOBECOM)*, 2010, pp. 1–6.
- [18] C. N. Manchón, G. E. Kirkelund, E. Riegler, L. P. B. Christensen, and B. H. Fleury, "Receiver architectures for MIMO-OFDM based on a combined VMP-SP algorithm," *arXiv: 1111.5848*, 2011.
- [19] Q. Guo and D. D. Huang, "EM-based joint channel estimation and detection for frequency selective channels using gaussian message passing," *IEEE Trans. Signal Process.*, vol. 59, no. 8, pp. 4030–4035, 2011.
- [20] P. Schniter, "A message-passing receiver for BICM-OFDM over unknown clustered-sparse channels," *IEEE J. Sel. Topics in Signal Process.*, vol. 5, no. 8, pp. 1462–1474, 2011.
- [21] C. Knievel, P. A. Hoeher, A. Tyrrell, and G. Auer, "Multi-dimensional graph-based soft iterative receiver for MIMO-OFDM," *IEEE Trans. Commun.*, vol. 60, no. 6, pp. 1599–1609, June 2012.
- [22] E. Riegler, G. E. Kirkelund, C. N. Manchón, M.-A. Badiu, and B. H. Fleury, "Merging belief propagation and the mean field approximation: A free energy approach," *IEEE Trans. Inf. Theory*, vol. 59, no. 1, pp. 588–602, Jan. 2013.
- [23] X. Zhang, P. Xiao, D. Ma, and J. Wei, "Variational-bayes-assisted joint signal detection, noise covariance estimation, and channel tracking in MIMO-OFDM systems," *IEEE Trans. Veh. Technol.*, vol. 63, no. 9, pp. 4436–4449, Nov. 2014.

- [24] D. D. Lin and T. J. Lim, "A variational inference framework for soft-in soft-out detection in multiple-access channels," *IEEE Trans. Inf. Theory*, vol. 55, no. 5, pp. 2345–2364, May 2009.
- [25] P. Schniter, "Joint estimation and decoding for sparse channels via relaxed belief propagation," in *Proc. of 44th Asilomar Conference on Signals, Systems and Computers. (ASILOMAR)*. IEEE, 2010, pp. 1055–1059.
- [26] M.-A. Badiu, G. E. Kirkelund, C. N. Manchón, E. Riegler, and B. H. Fleury, "Message-passing algorithms for channel estimation and decoding using approximate inference," in *Proc. IEEE Int. Symp. Inf. Theory (ISIT)*, 2012, pp. 2376–2380.
- [27] A. Drémeau, C. Herzet, and L. Daudet, "Boltzmann machine and mean-field approximation for structured sparse decompositions," *IEEE Trans. Signal Process.*, vol. 60, no. 7, pp. 3425–3438, July 2012.
- [28] F. Krzakala, A. Manoel, E. Tramel, and L. Zdeborová, "Variational free energies for compressed sensing," in *Proc. IEEE International Symposium on Information Theory (ISIT)*, June 2014, pp. 1499–1503.
- [29] M.-A. Badiu, C. Manchón, and B. Fleury, "Message-passing receiver architecture with reduced-complexity channel estimation," *IEEE Commun. Lett.*, vol. 17, no. 7, pp. 1404–1407, Jul. 2013.
- [30] T. P. Minka, "A family of algorithms for approximate Bayesian inference," Ph.D. dissertation, Massachusetts Institute of Technology, 2001.
- [31] S. Wu, L. Kuang, Z. Ni, J. Lu, D. D. Huang, and Q. Guo, "Expectation propagation approach to joint channel estimation and decoding for OFDM systems," in *Proc. IEEE Int. Conf. on Acoust., Speech and Signal Process. (ICASSP)*, Florence, Italy, May 2014, pp. 1941–1945.
- [32] J. T. Parker, P. Schniter, and V. Cevher, "Bilinear generalized approximate message passing—Part I: Derivation," *IEEE Trans. Signal Process.*, vol. 62, no. 22, pp. 5839–5853, Nov. 2014.
- [33] L. Schumacher, K. Pedersen, and P. Mogensen, "From antenna spacings to theoretical capacities-guidelines for simulating MIMO systems," in *Proc. IEEE Int. Symp. PIMRC*, 2002, pp. 587–592.
- [34] D. Ying, F. W. Vook, T. A. Thomas, D. J. Love, and A. Ghosh, "Kronecker product correlation model and limited feedback codebook design in a 3D channel model," in *Proc. of 2014 IEEE International Conference on Communications (ICC)*, Jun. 2014, pp. 5865–5870.
- [35] L. Dai, Z. Wang, and Z. Yang, "Spectrally efficient time-frequency training OFDM for mobile large-scale MIMO systems," *IEEE J. Sel. Areas Commun.*, vol. 3, no. 2, pp. 251–263, Feb. 2013.
- [36] P. Som, T. Datta, N. Srinidhi, A. Chockalingam, and B. Rajan, "Low-complexity detection in large-dimension MIMO-ISI channels using graphical models," *IEEE J. Sel. Topics in Signal Process.*, vol. 5, no. 8, pp. 1497–1511, Dec. 2011.
- [37] C. M. Bishop *et al.*, *Pattern recognition and machine learning*. New York: Springer, 2006.
- [38] J. Hu, H.-A. Loeliger, J. Dauwels, and F. Kschischang, "A general computation rule for lossy summaries/messages with examples from equalization," in *Proc. 44th Allerton Conf. Communication, Control, and Computing*, 2006, pp. 27–29.
- [39] M. R. Andersen, A. Vehtari, O. Winther, and L. K. Hansen, "Bayesian inference for spatio-temporal spike and slab priors," *arXiv:1509.04752*, 2015.
- [40] D. Hernández-Lobato, J. M. Hernández-Lobato, and P. Dupont, "Generalized spike-and-slab priors for Bayesian group feature selection using expectation propagation," *The Journal of Machine Learning Research*, vol. 14, no. 1, pp. 1891–1945, 2013.
- [41] J. M. Winn and C. M. Bishop, "Variational message passing," *The Journal of Machine Learning Research*, vol. 6, pp. 661–694, 2005.
- [42] B. M. Hochwald and S. ten Brink, "Achieving near-capacity on a multiple-antenna channel," *IEEE Trans. Commun.*, vol. 51, no. 3, pp. 389–399, Mar. 2003.

- [43] A. Van Den Bos, "Complex gradient and Hessian," in *IEE Proc. Vis., Image and Signal Processing*, vol. 141, no. 6. IET, 1994, pp. 380–383.
- [44] K. Kreutz-Delgado, "The complex gradient operator and the CR-calculus," *arXiv preprint arXiv:0906.4835*, 2009.